AWARD NUMBER: W81XWH-20-1-0677

TITLE: Development of a Dynamic Compression Fusion Device for Lower Extremity Salvage of the Diabetic Foot

PRINCIPAL INVESTIGATOR: Dr. David L. Safranski

CONTRACTING ORGANIZATION: MedShape, Inc., Atlanta, GA

REPORT DATE: September 2023

TYPE OF REPORT: Annual

PREPARED FOR: U.S. Army Medical Research and Development Command
Fort Detrick, Maryland 21702-5012

REPORT DOCUMENTATION PAGE

Form Approved
OMB No. 0704-0188

1. REPORT DATE	2. REPORT TYPE	3. DATES COVERED
September 2023	Annual	15Aug2022- 14Aug2023

4. TITLE AND SUBTITLE

Development of a Dynamic Compression Fusion Device for Lower Extremity Salvage of the Diabetic Foot

5a. CONTRACT NUMBER

5b. GRANT NUMBER
W81XWH-20-1-0677

5c. PROGRAM ELEMENT NUMBER

6. AUTHOR(S)

David L. Safranski, Ph.D.

E-Mail: David.Safranski@enovis.com

5d. PROJECT NUMBER

5e. TASK NUMBER

5f. WORK UNIT NUMBER

7. PERFORMING ORGANIZATION NAME(S) AND ADDRESS(ES)

MedShape, Inc.
1575 Northside Drive NW
Suite 440
Atlanta, GA 30318-5455

8. PERFORMING ORGANIZATION REPORT NUMBER

9. SPONSORING / MONITORING AGENCY NAME(S) AND ADDRESS(ES)

U.S. Army Medical Research and Development Command
Fort Detrick, Maryland 21702-5012

10. SPONSOR/MONITOR'S ACRONYM(S)

11. SPONSOR/MONITOR'S REPORT NUMBER(S)

12. DISTRIBUTION / AVAILABILITY STATEMENT

Approved for Public Release; Distribution Unlimited

13. SUPPLEMENTARY NOTES

14. ABSTRACT

Significant research findings during the research period include: development and testing of a dynamic compression device for use in challenging surgical foot procedures, such as fusion in the diabetic Veteran patient population. Testing results show superior mechanical performance in comparison to FDA-cleared competitor devices, including pull-out, static bending, cyclic bending, torsion, and the capacity for sustained compression in the face of simulated bone resorption. Additional project results include completion of all in vivo procedures for a large animal model for in vivo static and dynamic device evaluation featuring normal and low bone quality, as would be seen in more challenging patients. Implanted dynamic devices were observed to sustain compression over time, as assessed by serial radiograph examination. Microcomputed tomography was utilized to assess new bone formation at the joint fusion complex. Finally, mechanical testing of explanted joint complexes was demonstrated to assess integrity of joint fusion structures.

15. SUBJECT TERMS
Diabetic neuropathy, Charcot neuroarthropathy, arthrodesis, fusion, intramedullary, Nitinol, dynamic compression, biomechanics, midfoot, ovine model

16. SECURITY CLASSIFICATION OF:			17. LIMITATION OF ABSTRACT	18. NUMBER OF PAGES	19a. NAME OF RESPONSIBLE PERSON
a. REPORT	b. ABSTRACT	c. THIS PAGE			USAMRDC
Unclassified	Unclassified	Unclassified	Unclassified	39	19b. TELEPHONE NUMBER *(include area code)*

TABLE OF CONTENTS

1. Introduction

This technology development research project is directly applicable to diabetes, specifically the research of interventions to treat diabetes complications, such as Charcot neuroarthropathy. Charcot neuroarthropathy, also known as Charcot Foot, is an often painless, progressive, inflammatory, destructive degenerative disease of the midfoot and ankle. It is characterized by joint dislocations and fractures that result in deformities of the foot. These deformities often lead to ulceration, infection, and lower limb amputation. The overarching challenge in correcting Charcot foot deformities involves addressing two clinical issues: poor bone quality and harsh loading conditions from neuropathic patients. With Charcot foot, enhanced osteoclastic activity drives bone resorption and osteolysis, which loosens current fusion devices. With loosening, the compressive forces of current devices are lost, thus bone-bone contact decreases and micromotion occurs, preventing fusion and leading to implant breakage. We present the use of the superelastic alloy nickel-titanium (NiTi or nitinol), which has a large reversible strain recovery. This large strain recovery allows for a NiTi-based medical device to dynamically adapt to bone resorption by continuing to apply a compressive force to maintain bone-bone contact. This effectively creates a device that post-operatively responds automatically to changes in the bone healing environment during fusion. The objective of this technology development proposal is to develop a dynamic compression midfoot fusion device capable of enhanced bone fusion for salvage reconstruction of the diabetic Charcot foot. The central hypothesis is that a NiTi-based fusion device can enhance bone fusion by dynamically adapting to bone resorption to maintain bone-on-bone interfacial compression compared to a static competitor's device. Aim 1: Verify the prototype device's mechanical performance compared to an FDA-cleared competitor's device. Aim 2: Validate the prototype device's ability to apply dynamic compression in vivo using an ovine hindlimb fusion model. In Aim 1, the mechanical performance of the prototype fusion device will be compared against a competitor's device previously cleared by the FDA using relevant industry standards to ensure the safety of the device. These studies will generate the necessary mechanical data for FDA submission and further demonstrate the ability of dynamic sustained compression to adapt to bone resorption in small bones of the foot (Major Task 1). In Aim 2, the ability of the prototype device to enhance fusion via dynamic compression will be validated using an ovine hindlimb model. This study will ensure the efficacy of the device to enhance fusion in vivo compared to a static device. A control group of sheep with normal bone quality will undergo a multi-joint fusion of the hindlimb to simulate midfoot fusion. Radiographic and CT imaging, mechanical testing, and histological evaluation of the fusion site will be used to assess the efficacy of the prototype device to promote fusion under normal biological conditions (Major Task 2). To mimic Charcot foot, low bone quality will be induced in a separate group of sheep, followed by multi-joint fusion of the hindlimb. Radiographic and CT imaging, mechanical testing, and histological evaluation of the fusion site will be used to assess the efficacy of the dynamic prototype device to promote fusion under very challenging biological conditions (Major Task 3).

2. Keywords

Diabetic neuropathy, Charcot neuroarthropathy, arthrodesis, fusion, intramedullary, Nitinol, dynamic compression, biomechanics, midfoot, ovine model

3. Accomplishments

3.1 Specific Aim 1: Verify the prototype device's mechanical performance compared to an FDA-cleared competitor's device.

3.1.1 Major Task 1: Verify the prototype device's mechanical performance compared to an FDA-cleared competitor's device.

Subtask 1-Axial Pullout Test

Year 1 Accomplishments: The protoype dynamic device went through multiple rounds of design iterations, especially in regards to its threaded end for fixation in cancellous bone and its overall diameter. Initially, the prototype device had a diameter close to 5 mm and transverse screws for fixation in bone; however, this would not have met the criteria for substantial equivalency for pull-out strength and bending strength. Thus, a second version of the dynamic prototype was developed with a threaded end for fixation in the proximal metatarsal and a slot for a transverse screw for fixation in the calcaneus to reconstruct the lateral column of the foot. The threaded end of the prototype device was designed with a taper to closely mimic the gradual taper of the proximal metatarsal intramedullary canal. The overall diameter was increased to 7 mm to increase the bending strength and to be comparable to static predicate devices. A CAD model of the final dynamic prototype device and a manufactured prototype device is shown in Figure 1.

The first metric to examine was the pull-out force of the prototype device compared to a static predicate device (Synthes Midfoot Fusion Bolt, 140 mm) (Figure 2). A finalized protocol has been developed and added to

the MedShape Design History File in compliance with 21 CFR 820.30(j) and 21 CFR 820.40, ED-50388-00, DynaNail Mini Tapered Hybrid Pull-Out Testing Protocol, which follows ASTM F543 to determine the pull-out strength of medical bone screws. Briefly, the static predicate device or the dynamic prototype device is inserted into a synthetic bone block (Sawbones 20PCF), then a force is applied to the device via a pin to drive it in the opposite direction of its insertion (Figure 3). This allows for separation and independent examination of both fixation methods at each end of the devices. From the pictures, the left side of the device is noted as the cortical fixation as it fixates into cortical bone either with threads or a transverse screw. The right side of each device consists of thread length of 16 mm and is noted as the cancellous fixation. The pull-out force for each fixation method for each device is shown in Figure 4 (n=10/device). The cortical and cancellous pull-out force for the dynamic prototype device is greater than the static predicate device. While the static predicate device has fixed thread forms on each end of the device, the transverse screw tested for the cortical fixation of the dynamic prototype device was 14 mm in length. This represents the smallest transverse screw to be offered, thus the worst-case scenario. In practical application, the transverse screw will match the width of the calcaneus, thus it is expected that the pull-out force would be significantly higher.

Figure 1. (left) CAD model of final dynamic prototype device. (right) Manufactured dynamic prototype device.

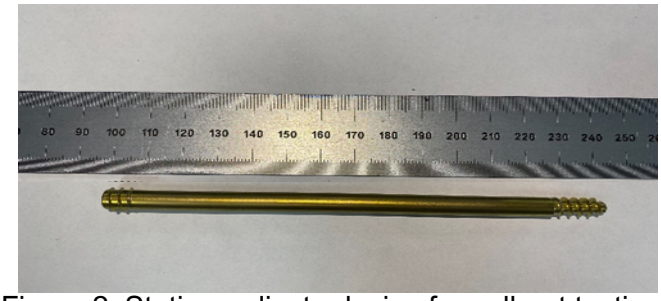

Figure 2. Static predicate device for pull-out testing.

Figure 3. Test setup for determining pull-out force of each device.

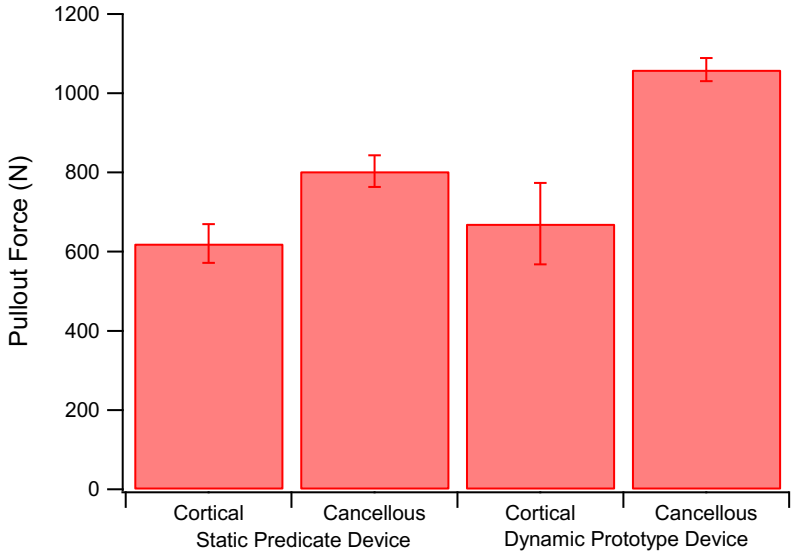

Figure 4. Pull-out force for static predicate device and dynamic prototype device.

Year 2 Accomplishments: A formalized report, ED-50450-00, DynaNail Mini Tapered Hybrid Pull-out Testing Report was added to the MedShape Design History File in compliance with 21 CFR 820.30(j) and 21 CFR 820.40, based on the data from Figure 4. Based upon prior protocol, ED-50388, testing was performed in synthetic anatomic models of the metatarsal and calcaneus. To simulate this procedure, the predicate device and the dynamic prototype device were inserted posteriorly into a calcaneus model and were fixated into the bone with either cortical threads (predicate) or a headless transverse screw (prototype) (Figure 5). The cancellous threads of both the predicate device and the dynamic prototype device were implanted into a metatarsal model through the proximal end of the bone (Figure 5). Samples were mounted in an Instron mechanical testing system and a force applied at 5mm/min to remove the devices from the synthetic bone. Max force was recorded (n≥9/group).

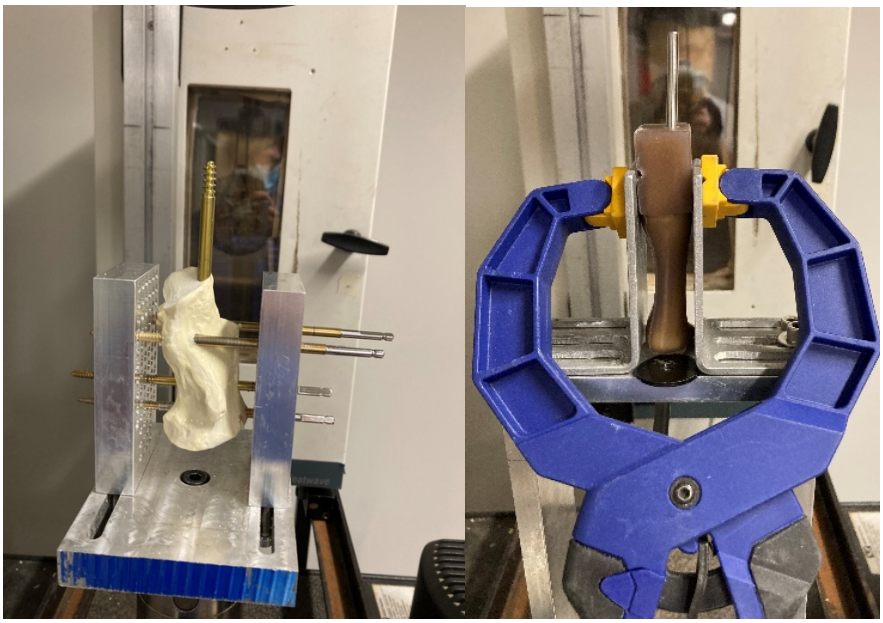

Figure 5. Test setup for determining pull-out force in (left) synthetic calcaneus and (right) synthetic metatarsal.

The predicate cortical threads had an average pushout strength of 915.9 ± 110 N, and the prototype device's headless transverse screw produced an average pushout strength of 2036.8 ± 161 N. After running the data through a t-test, it was determined that the prototype produces a significantly higher pull-out strength with the headless transverse screw than the predicate device does with its cortical threads ($p<0.01$). The predicates' cancellous threads had an average pushout strength of 677.7 ± 150 N, and the prototype's cancellous threads had an average pushout strength of 713.9 ± 130.7 N. While the cancellous threads of the prototype did produce

a larger average pushout strength than those of the predicate, the difference is not statistically significant (Figure 6).

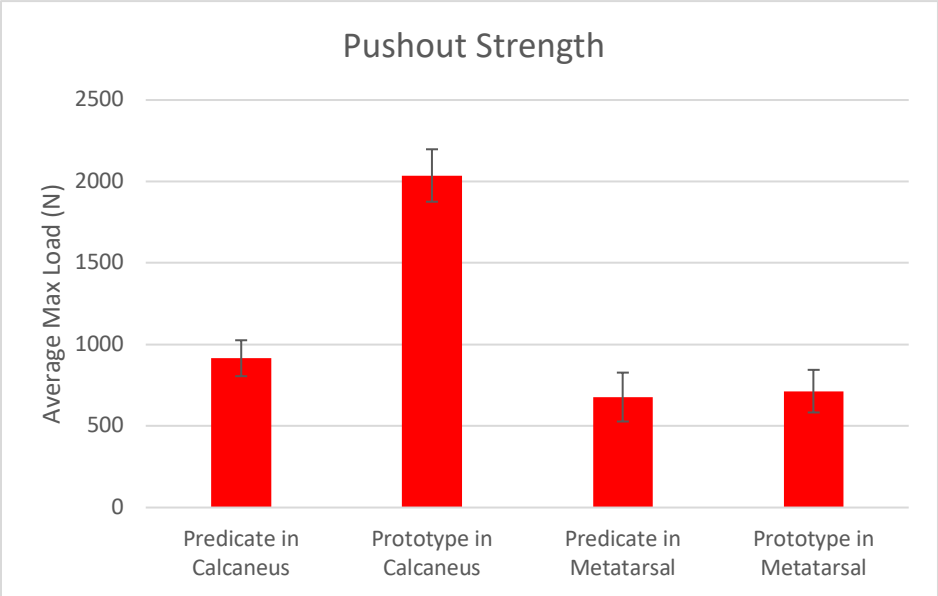

Figure 6. Max pushout force for predicate and prototype device in synthetic bones.

Training and Professional Development Opportunities: Nothing to Report
Dissemination of Results: Results were presented at the Orthopaedic Research Society Meeting in Tampa, FL, in February 2022, “Biomechanical Comparison in Synthetic Bone of Dynamic Versus Static Intramedullary Fixation Devices for Midfoot Arthrodesis”.
Future Plan: None. Testing and reports are finished.
Status: 100% Complete.

Subtask 2-Static Bend Test
Year 1 Accomplishments: A finalized protocol has been developed and added to the MedShape Design History File in compliance with 21 CFR 820.30(j) and 21 CFR 820.40, ED-50413-00, DynaNail Mini Tapered Hybrid and Predicate Static 4 Point Bend Testing Protocol, which follows ASTM F1264 to determine the static 4-point bending performance of intramedullary devices. The dynamic prototype device with an overall length of 140 mm was compared against a static predicate device (Wright Salvation Beam) with an overall length of 140 mm to represent the worst-case bending scenario. A picture of the 4-point setup in shown in Figure 7 on a MTS Mini Bionix load frame. Samples were tested past their yield point to permanently deform the specimens in bending (n=8/device). Exemplary bending curves are shown in Figure 8 for each device. Bending stiffness, yield moment and yield force were calculated for each test following ASTM F1264. The bending stiffness, yield moment, and yield force were greater for the dynamic device than the static predicate device (Figures 9,10,11).

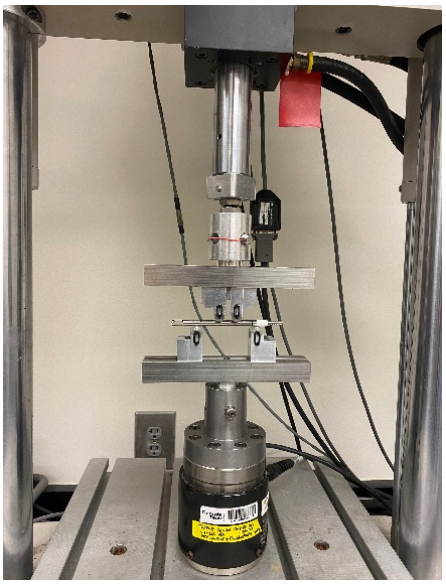

Figure 7. 4-point bending test setup.

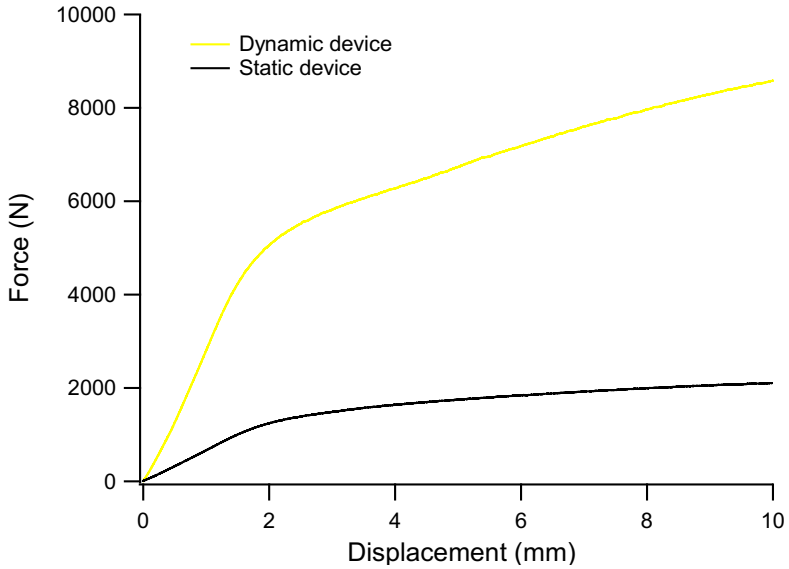

Figure 8. Representative bending curves for each device.

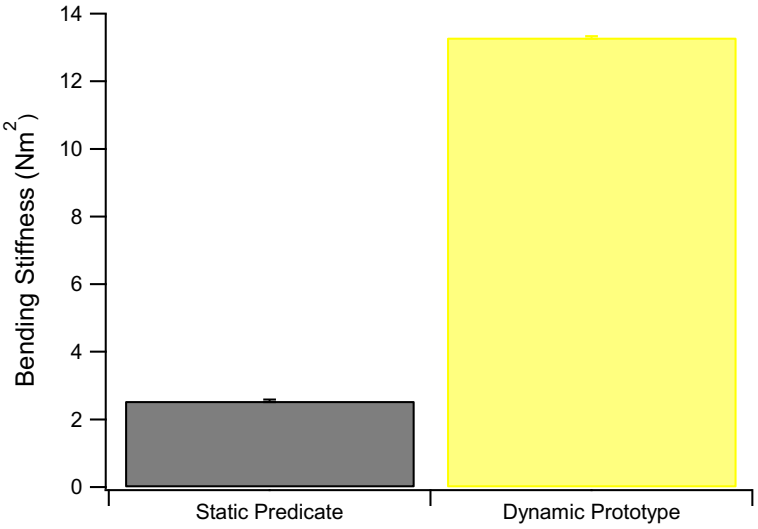

Figure 9. Bending stiffness for static predicate device and dynamic prototype device.

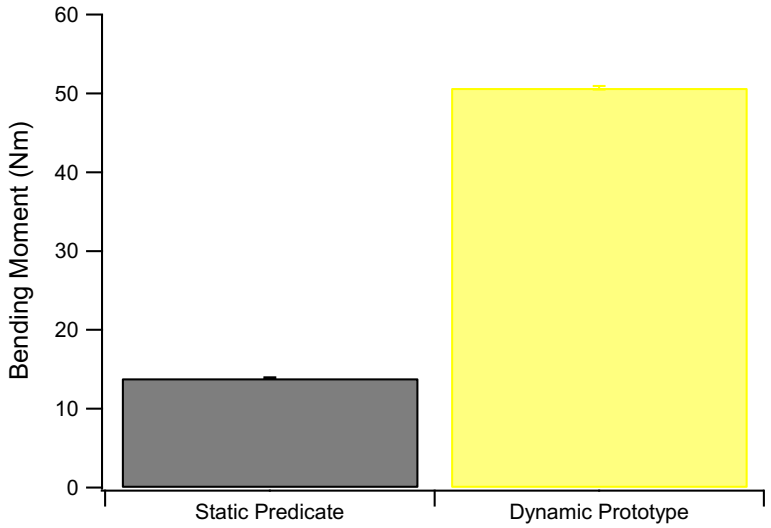

Figure 10. Bending moment for static predicate device and dynamic prototype device.

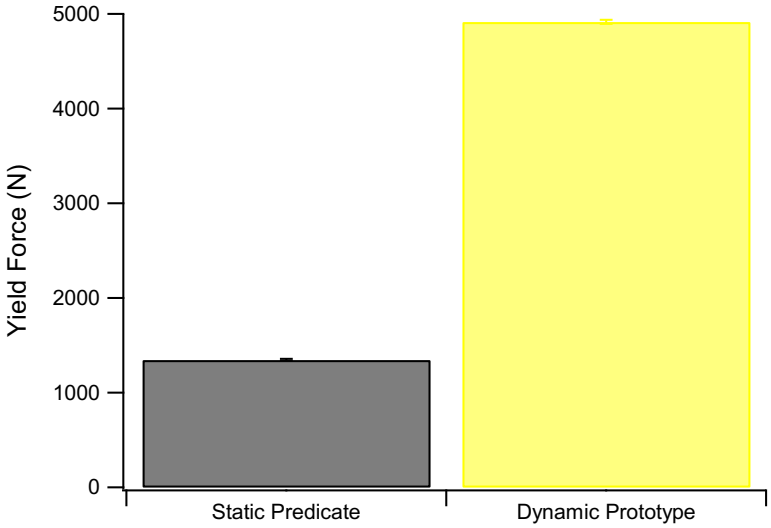

Figure 11. Yield force for static predicate device and dynamic prototype device.

Year 2 Accomplishments: A finalized report, ED-50452, DynaNail Mini Tapered Hybrid Static 4pt Testing Report was generated and added to the MedShape Design History File in compliance with 21 CFR 820.30(j) and 21 CFR 820.40. The dynamic prototype showed significantly higher bending stiffness, bending moment, and yield force, compared to the predicate device ($p<0.001$).
Training and Professional Development Opportunities: Nothing to Report
Dissemination of Results: Results were presented at the Orthopaedic Research Society Meeting in Tampa, FL, in February 2022, “Biomechanical Comparison in Synthetic Bone of Dynamic Versus Static Intramedullary Fixation Devices for Midfoot Arthrodesis”.
Future Plan: None. Testing and reports are finished.
Status: 100% Complete.

Subtask 3-Static Torsion Test
Year 1 Accomplishments: A draft protocol has been developed following ASTM F1264 to determine the torsional stiffness of intramedullary devices. A set of custom grips have been designed and machined (Figure 12, Figure 13) to grip the static predicate device and the dynamic prototype device for torsion testing at Colorado State University in a MTS Mini Bionix load frame. The MTS load frame at Georgia Tech does not have pneumatic grips, thus it is unable to apply the necessary forces for holding these custom grips.

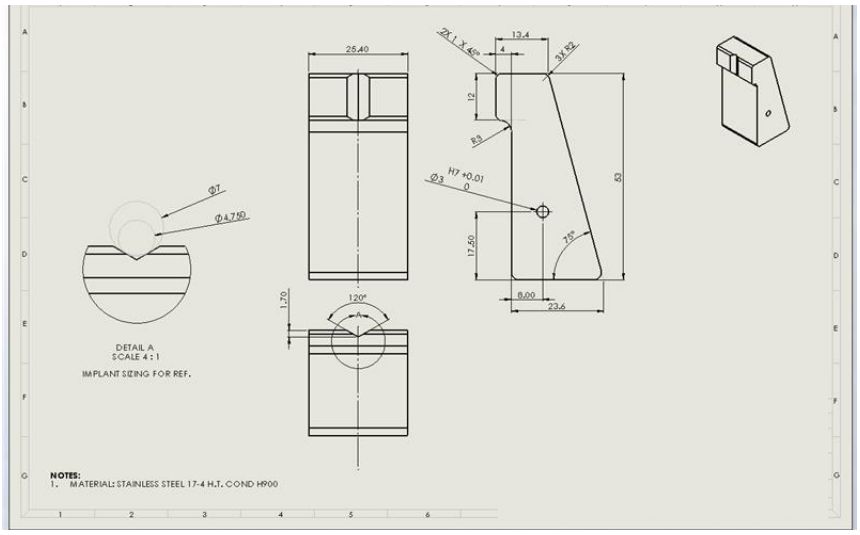

Figure 12. Drawing of grips for torsion testing.

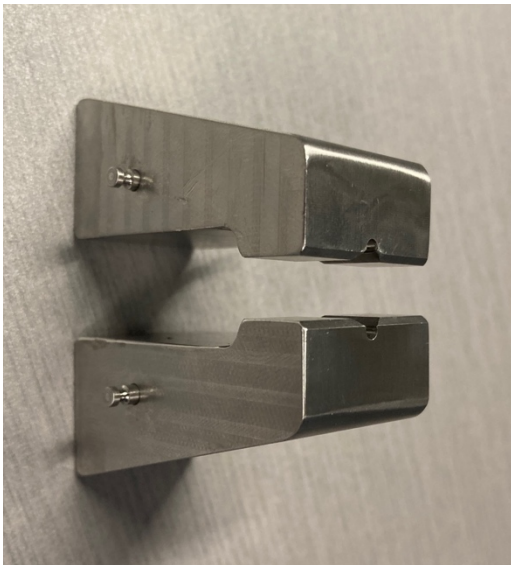
Figure 13. Machined set of grips for torsion testing.

Year 2 Accomplishments: Following ASTM F1264, a protocol, ED-50422 DynaNail Mini Tapered Hybrid and Predicate Torsional Testing Protocol, was finalized and added to the MedShape Design History File in compliance with 21 CFR 820.30(j) and 21 CFR 820.40. Subsequent testing was carried out according to the protocol, where the predicate device and dynamic prototype device were torqued at a rate of 5°/min to 5° or until a straight-line portion of the torque rotation curve (n=10/device). Exemplary images of the test setup are shown in Figure 14, and exemplary raw data is shown in Figure 15 for each device. The torsional stiffness of the dynamic prototype device (2236±9.10 N*mm/º) was almost 5 times as stiff as the static predicate device (472±3.53 N*mm/º) ($p<0.01$) (Figure 16). A finalized report, ED-50440 DynaNail Mini Tapered Hybrid Torsional Testing Report, was added to the MedShape Design History File in compliance with 21 CFR 820.30(j) and 21 CFR 820.40.

Figure 14. (left) Upper and lower pneumatic grips with custom torsion fixtures. (center) Inset view with predicate device clamped in fixture for torsion testing. (right) Inset view with prototype device clamped in fixture for torsion testing.

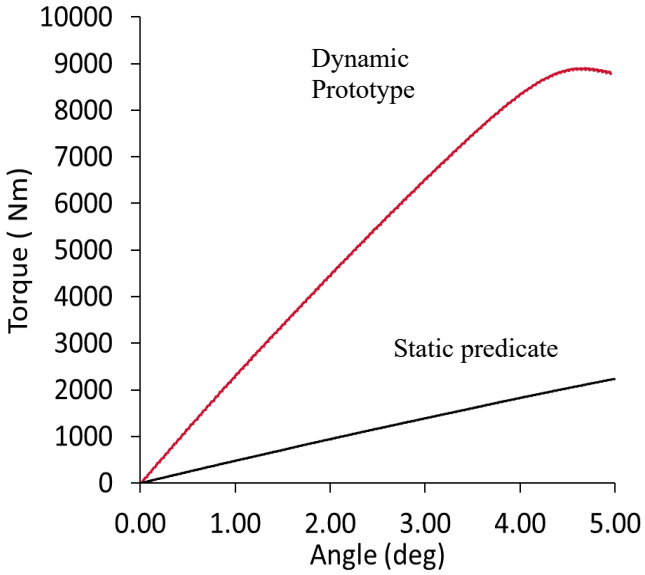

Figure 15. Exemplary raw data from torsion test.

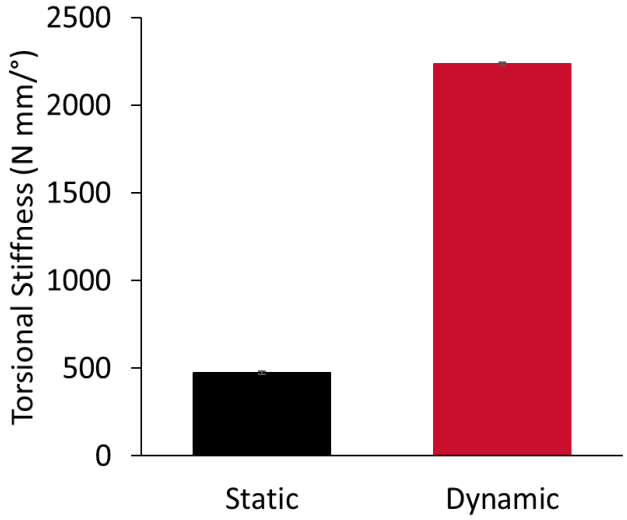

Figure 16. Torsional stiffness for static predicate and dynamic prototype device.

Training and Professional Development Opportunities: Nothing to Report
Dissemination of Results: Results were presented at the Orthopaedic Research Society Meeting in Tampa, FL, in February 2022, “Biomechanical Comparison in Synthetic Bone of Dynamic Versus Static Intramedullary Fixation Devices for Midfoot Arthrodesis”.
Future Plan: None. Testing and reports are finished
Status: 100% Complete.

Subtask 4-Cyclic Bend Test
Year 1 Accomplishments: A finalized protocol has been developed and added to the MedShape Design History File in compliance with 21 CFR 820.30(j) and 21 CFR 820.40, ED-50411-00, DynaNail Mini Tapered Hybrid and Predicates Cyclic Bend Testing Protocol, which follows ASTM F1264. After determining the yield force from Subtask 3, the static predicate device and dynamic prototype device were loaded cyclically at 5 Hz at decreasing loads starting at 100% of the yield force to determine the run-out force. The test setup utilizes the same fixtures as Figure 7. Testing has shown that the static predicate device has a run-out of 1 million cycles near 75% of its yield force.

Year 2 Accomplishments: Cyclic testing was completed for the predicate (Wright Beam) and dynamic prototype device. The predicate device reached a runout of 1010 N at 1 million cycles, while the dynamic prototype device had a runout load of 2454 N at 1 million cycles. The cyclic results are shown in Figure 17. A formal testing report, ED-560449 DynaNail Mini Tapered Hybrid Cyclic Bend Test Report, has been added to the MedShape Design History File in compliance with 21 CFR 820.30(j) and 21 CFR 820.40.

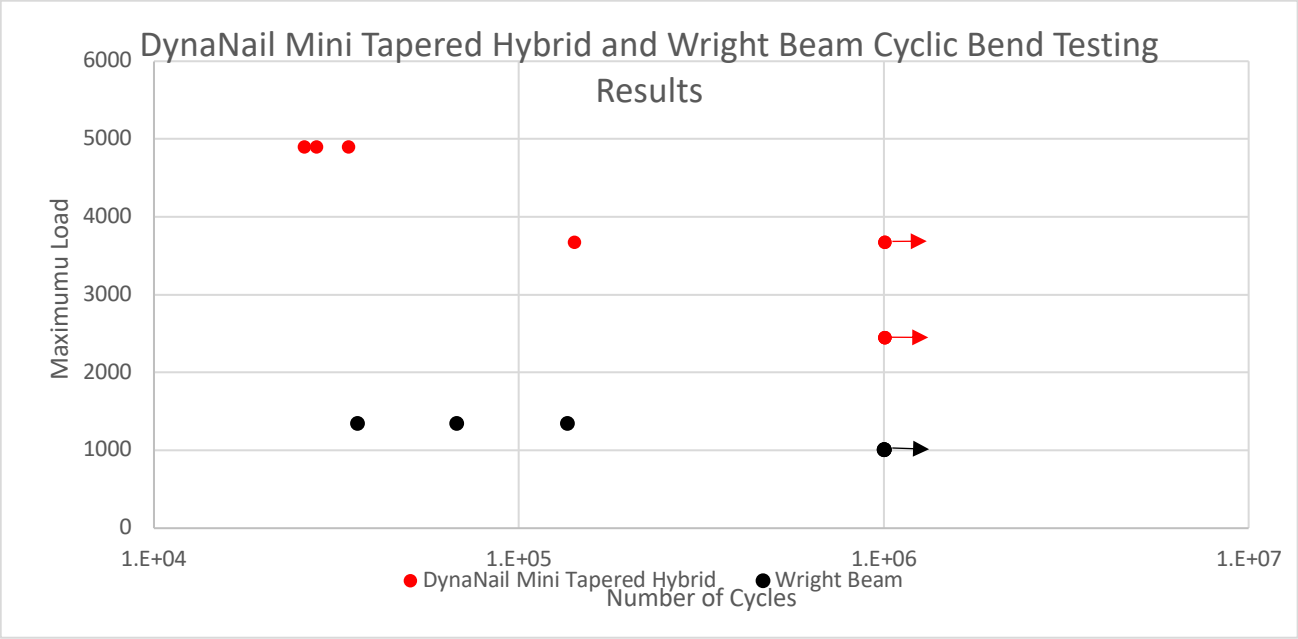

Figure 17. Cyclic performance of prototype and predicate device.

Training and Professional Development Opportunities: Nothing to Report
Dissemination of Results: Results were presented at the Orthopaedic Research Society Meeting in Tampa, FL, in February 2022, “Biomechanical Comparison in Synthetic Bone of Dynamic Versus Static Intramedullary Fixation Devices for Midfoot Arthrodesis”.
Future Plan: None. Testing and reports are finished.
Status: 100% Complete.

Subtask 5-Simulated Bone Resorption Test
Year 1 Accomplishments: A finalized protocol has been developed and added to the MedShape Design History File in compliance with 21 CFR 820.30(j) and 21 CFR 820.40, ED-50403-00, DynaNail Mini Tapered Hybrid and Predicates Resorption Testing Protocol. The test setup consists of implanting the predicate device or the dynamic prototype device through a load cell, a custom stage to mimic bone resorption, and then fixated in two synthetic bone blocks (20 PCF) (Figure 18). The entire apparatus is placed inside a thermal chamber held at

37°C to mimic body temperature, as biological resorption would occur over weeks to months post-implantation following device temperature equilibration to body temperature. The stage is lowered to apply slack to the system and the change in compressive load is recorded (n=8/device). The compressive load as a function of simulated resorption is shown in Figure 19. The static predicate device (Wright Beam 7 x 140 mm) loses all compression within 1 mm of simulated resorption, while the dynamic prototype device (7 x 140 mm) sustains compression for 7 mm of simulated bone resorption. Thus, the dynamic prototype device has greater capacity to adapt to bone resorption, which is critical in diabetic patients with Charcot.

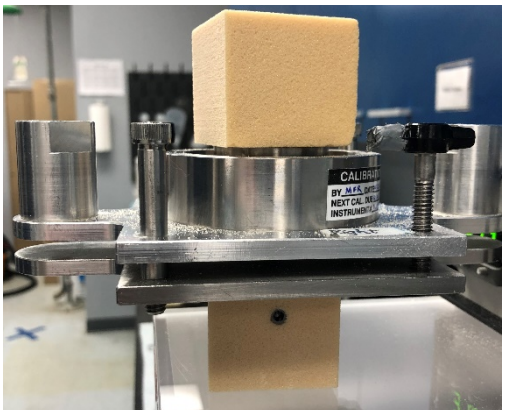

Figure 18. Resorption assembly for the dynamic prototype device showing the upper synthetic bone block, load cell, custom resorption stage, and lower synthetic bone block.

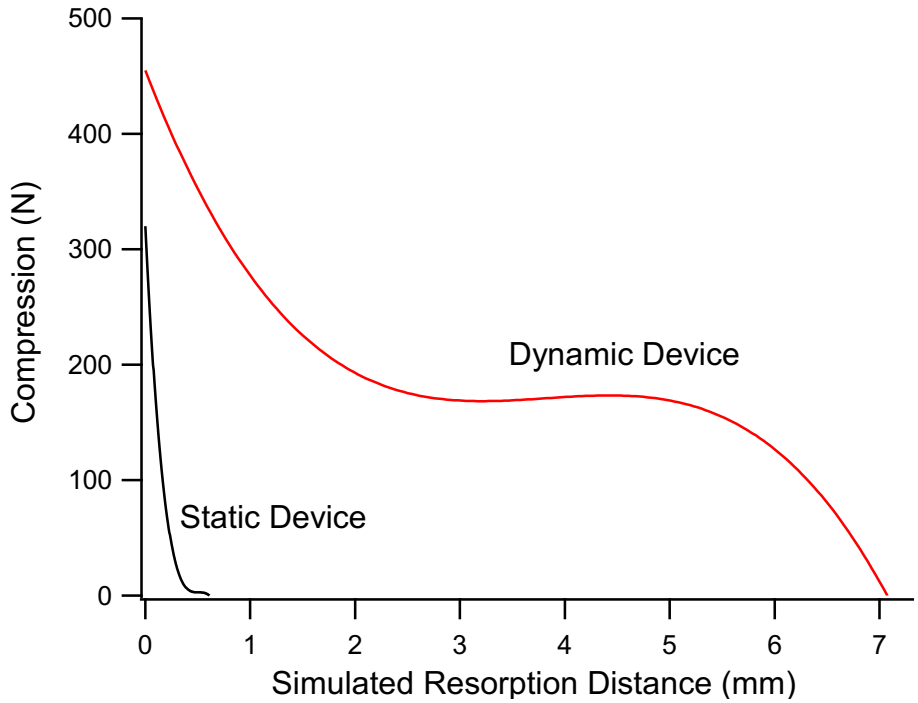

Figure 19. Compression profile during simulated resorption for the static predicate device and dynamic prototype device. Both devices have equivalent overall length of 140 mm.

Year 2 Accomplishments: Additional testing of the dynamic prototype device at device lengths of 110 mm, 120 mm, and 130 mm was performed to ensure that their ability to adapt to simulated bone resorption is equivalent to or greater than the static predicate device. Following the established protocol from Year 1, the additional devices underwent simulated bone resorption testing (Figure 20). The resorption capacity ranges from 5.5 mm to 7.0 mm as the device length increases from 110 mm to 140 mm. The 130 mm and 140 mm prototype devices have the same internal nitinol element, thus have similar resorption capacity near 7 mm.

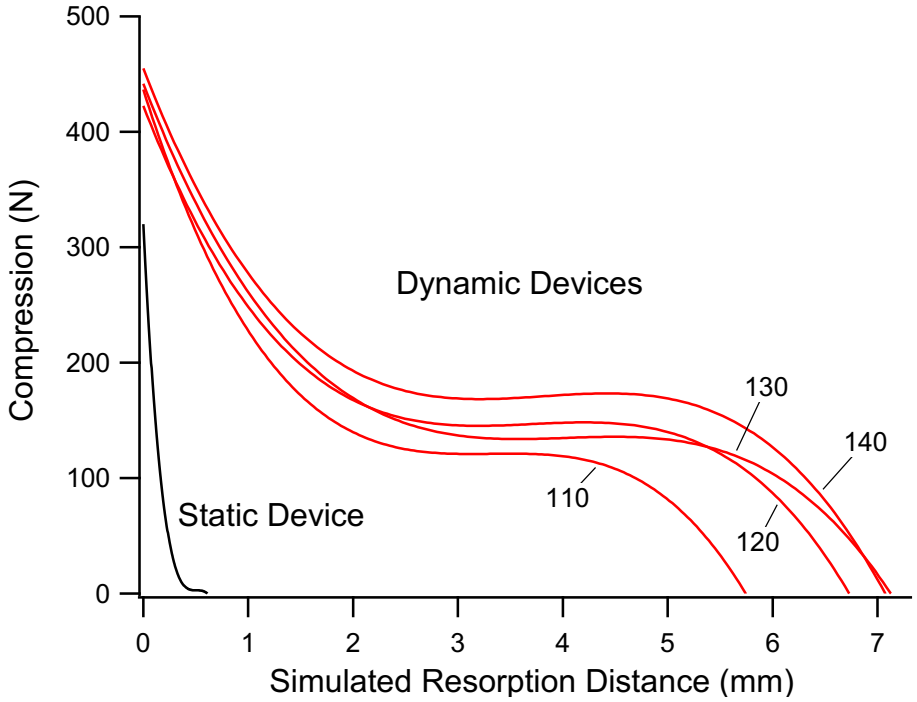

Figure 20. Compression profile during the simulated resorption for varying size of dynamic prototype.

Year 3 Accomplishments: A formalized test report was generated and added to the MedShape Design History File in compliance with 21 CFR 820.30(j) and 21 CFR 820.40 in the second quarter of 2023, ED-50404-00, DynaNail Mini Tapered Hybrid Resorption Testing Report.
Training and Professional Development Opportunities: Nothing to Report
Dissemination of Results: Results were presented at the Orthopaedic Research Society Meeting in Tampa, FL, in February 2022, “Biomechanical Comparison in Synthetic Bone of Dynamic Versus Static Intramedullary Fixation Devices for Midfoot Arthrodesis”.
Future Plan: None.
Status: 100% Complete.

Subtask 6-Manufacture and Assembly
Year 1 Accomplishments: Finalized manufacturing protocols have been developed and approved through the MedShape quality management system, ED-10928-00, Implant Assembly, DynaNail Mini Tapered Hybrid, which details assembly of the internal implant components for the dynamic prototype device (Figure 21), and ED-10929, Nail Assembly, DynaNail Mini Tapered Hybrid, which details assembly of the prototype device with its nail guide for surgical delivery (Figure 22). An exemplary fully assembled device is shown in Figure 23 with the device attached to its nail guide. All device components were manufactured, inspected, and assembled in compliance with the current Good Manufacturing Practices established by the US FDA. In order to keep Specific Aim 2 on schedule, the manufacture and assembly of devices for Specific Aim 2 were prioritized first. All devices for the animal study in Specific Aim 2 have been assembled and packaged.

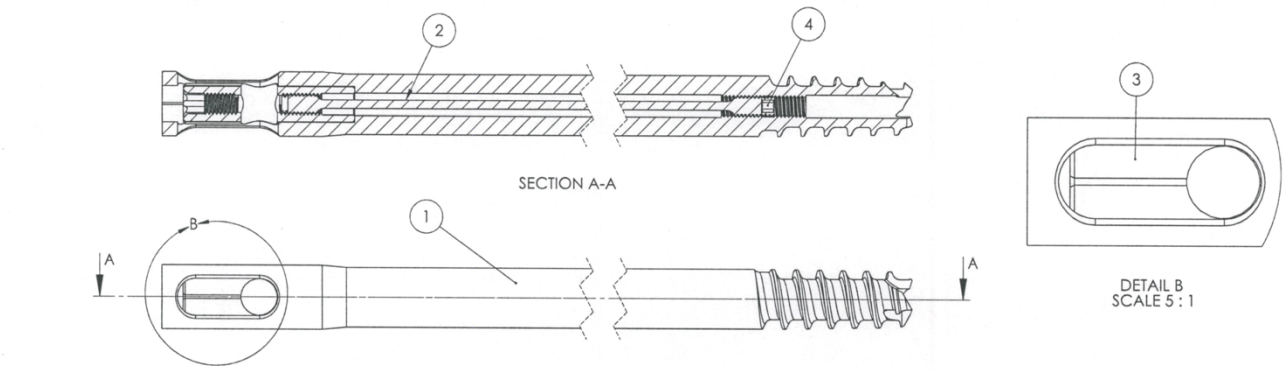

Figure 21. Manufacturing schematic for assembly of internal components of dynamic prototype device.

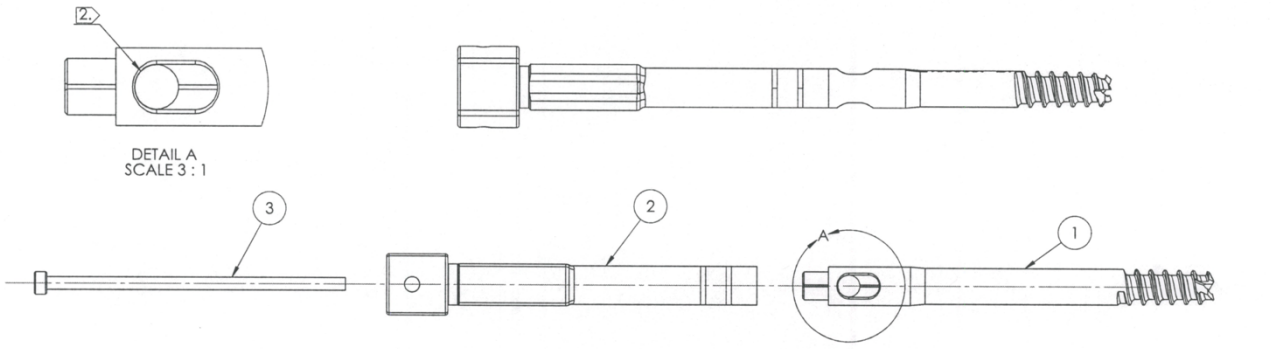

Figure 22. Manufacturing schematic for assembly of dynamic prototype device and nail guide.

Figure 23. Fully assembled device with nail guide on left side and dynamic prototype device on right side.

Year 2 Accomplishments: The remaining dynamic prototype devices for packaging and sterilization testing were assembled per manufacturing and assembly protocols. This task was completed in December 2021.
Training and Professional Development Opportunities: Nothing to Report
Dissemination of Results: Nothing to Report
Future Plan: None. Task completed.
Status: 100% Complete.

Subtask 7-Packaging and Sterilization
Year 1 Accomplishments: Packaging has been designed following, ED-10947, Item Master, DynaNail Mini Hybrid Tapered, and added to the MedShape Design History File in compliance with 21 CFR 820.30(j) and 21 CFR 820.40. Figure 24 and Figure 25 detail the packaging components for the dynamic prototype device. These have been adapted from prior MedShape products of similar size and weight.

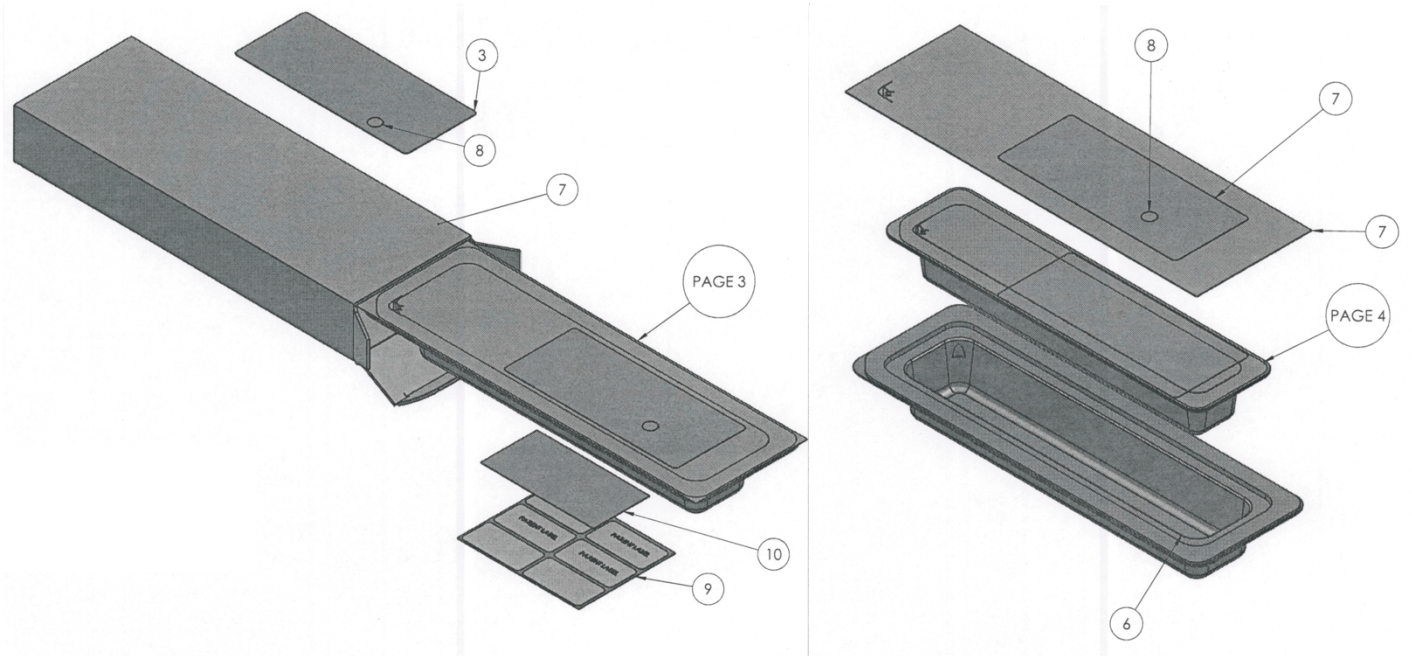

Figure 24. (left) Outer packaging components including label, carton, instructions for use, inner tray assembly. (right) Inner tray assembly components including sterilization indicator, label, outer lid, inner tray and outer tray.

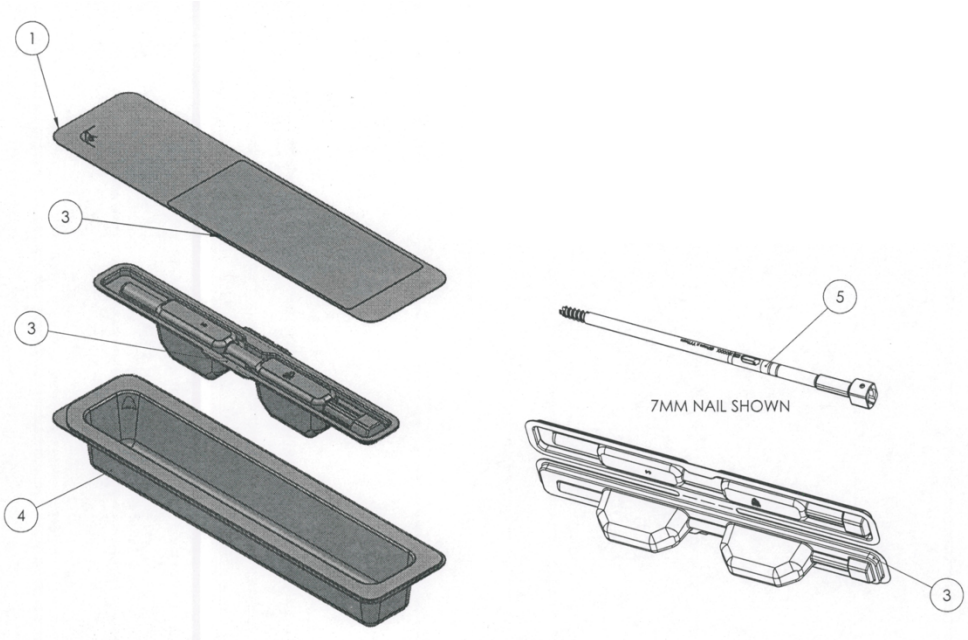

Figure 25. (left) Inner tray components including inner lid, clamshell, and inner tray. (right) Clamshell and assembled dynamic prototype device.

Year 2 Accomplishments: The outer and inner tray packaging was received, and devices for sterilization testing were assembled and packaged in December 2021. The packaging is shown in Figure 26 and Figure 27 with an assembled device for the sterilization testing, including both the outer and inner tray components.

Figure 26. (left) Outer carton with labeling. (Right) Inner tray assembly from Figure 24.


Figure 27. Bottom view of inner tray with dual layer packaging with a fully assembled device from Figure 25.

Following assembly and packaging, devices underwent a sterilization adoption to the existing Method VDmax validation from prior MedShape product according to ISO 11137-2: Sterilization of Health Care Products-Radiation-Establishing the sterilization dose-Method VDmax dose audit. First, bioburden and recovery testing was performed on the prototype device to determine the number of colony forming units after packaging and assembly. A bioburden recovery validation was conducted on five devices using the exhaustive recovery method. The recovery efficiency was unable to be determined, as the bioburden was too low to be quantified. Thus, a second bioburden recovery validation was conducted on five devices using the inoculated recovery method. The recovery efficiency of 80.2% was determined and utilized for the bioburden results. The total bioburden was found to be 7.5 colony forming units per device. The historical verification dose of 8 kGy was used for the dose audit as 7.5 colony forming units per device was below historical bioburden values. The Method VDmax validation procedure has a 1,000 colony forming units per device limit, thus the bioburden results are substantially below the limit. After the verification dose, a sterility test was conducted on 10 devices, and 0 devices were positive, which met the acceptance criteria of no more than one positive device per 10 sample devices. In accordance with ISO 11137-2: Method VDmax, statistical verification was successfully completed since not more than one positive sterility test culture was observed after irradiation at the determined verification dose for the lot tested. The average bioburden was less than 1,000 organisms and statistical verification of the bioburden resistance was accepted. As such, the dynamic prototype has passed the dose audit based on the criteria established by the original validation of prior MedShape devices. Additionally, it is recommended that the dynamic prototype be considered a sterilization family member with prior MedShape device validation based on the completion of the dose audit. Routine sterilization of subsequent manufacturing lots will require

demonstration, through dosimetry, that this 10^{-6} sterility assurance dose has been achieved at the point of minimum absorbed dose in each irradiation carrier load. In addition, dose mapping of routine production loads, to determine reproducible points of minimum absorbance, and calibration of physico-chemical dosimeters, to be located at those points, will be required to demonstrate the degree of process control required for dosimetric release of sterilized products. These procedures will be the responsibility of the sponsor and sterilization service provider Sterigenics. To substantiate the continued validity of 25 kGy dose as a 10^{-6} sterility assurance level (SAL) dose, verification dose audits must continue to be performed according to an established schedule, as specified in ISO 11137-1. A minimum dose of 25 kGy supports the release of the dynamic prototype device, and the dose was statistically verified since not more than one positive sterility test culture was observed after irradiation. In addition, the average bioburden was less than 1,000 microorganisms, and the sterilization dose of 25kGy is the 10^{-6} SAL for the dynamic prototype device.

Year 3 Accomplishments: Packaging testing started in September 2022 and was successfully completed in November 2022. This testing assessed adhesive failure of packaging seals and followed ASTM F88 – Seal Tensile Strength. This testing was completed before the end of the performance period as necessary for regulatory submission to ensure package integrity.
Training and Professional Development Opportunities: Nothing to Report
Dissemination of Results: Nothing to Report
Future Plan: None.
Status: 100% Complete.

Subtask 8-Regulatory Documentation
Year 1 Accomplishments: Design documents have been developed and approved through the MedShape quality management system, ED-50377 Product development plan, DynaNail Mini Hybrid Tapered, and ED-50378 Design Record, DynaNail Mini Hybrid Tapered.
Year 2 Accomplishments: The following GLP test protocols and reports were approved within the MedShape quality management system for regulatory submission: ED-50450 DynaNail Mini Tapered Hybrid Pull-Out Testing Report, ED-50403 DynaNail Mini Tapered Hybrid and Predicates Resorption Testing Protocol, ED-50452 DynaNail Mini Tapered Hybrid Static 4pt Testing Report, ED-50449 DynaNail Mini Tapered Hybrid Cyclic Bend Testing Report, ED-50440 DynaNail Mini Tapered Hybrid Torsional Testing Report, ED-10947 DynaNail Mini Tapered Hybrid Item Master, ED-50422 DynaNail Mini Tapered Hybrid and Predicate Torsional Testing Protocol, and TR-EAS-2022-0526 Product Adoption of 7x140mm DynaNail Mini Tapered Hybrid.
Training and Professional Development Opportunities: Nothing to Report
Dissemination of Results: Nothing to Report
Year 3 Accomplishments: Design documents as well as GLP test reports have been developed and added to the MedShape Design History File in compliance with 21 CFR 820.30(j) and 21 CFR 820.40, including ED-50379-00, Risk Management Document - Design DynaNail Mini Hybrid Tapered and ED-50380-00, Design Verification Test Plan DynaNail Mini Tapered Hybrid, and ED-50404-00, DynaNail Mini Tapered Hybrid Resorption Testing Report
Future Plan: A design phase review meeting for the prototype device has been scheduled for September 2023. Upon receipt of final in vivo testing data from Specific Aim 2 and 3, all design-related documentation will be compiled and submitted for clearance via a Traditional 510(k) submission with the US FDA with clearance expected to occur in early 2024, followed by anticipated design transfer and product launch activities in 2024.
Status: 85% Complete

3.2 Specific Aim 2: *Validate the prototype device's ability to apply dynamic compression in vivo using an ovine hindlimb fusion model.*
Subtask 1-Local IRB/IACUC Approval
Year 1 Accomplishments: Protocol #1199-MedShape-Development of a dynamic compression fusion device for lower extremity salvage of the diabetic foot was approved September 1, 2020 by the Colorado State University Institutional Animal Care and Use Committee (IACUC). An amendment was approved on March 1, 2021, and another amendment was approved on July 30, 2021 for the same protocol.

Year 2 Accomplishments: An additional amendment was approved on April 15, 2022 by Colorado State University.
Training and Professional Development Opportunities: Nothing to Report
Dissemination of Results: Nothing to Report

Future Plan: No further IACUC amendments are anticipated.
Status: 100% Complete

Subtask 2-ACURO Approval
Year 1 Accomplishments: ACURO protocol PR191551 entitled, MedShape-Development of a dynamic compression fusion device for lower extremity salvage of the diabetic foot, was approved September 24, 2020. Additional ACURO approval was granted on April 14, 2021, and on August 6, 2021 for amendments to the original protocol for bone labels and additional imaging.

Year 2 Accomplishments: Further ACURO approval was granted on May 9, 2022, for amendment.
Training and Professional Development Opportunities: Nothing to Report
Dissemination of Results: Nothing to Report
Future Plan: No further ACURO amendments are anticipated.
Status: 100% Complete

*3.2.1 **Major Task 2:** Validate the prototype device's ability to apply dynamic compression in vivo using an ovine hindlimb fusion model with normal bone quality.*

Subtask 1-Fusion Surgery
Year 1 Accomplishments: This study utilized a skeletally mature Rambouillet Cross ewe due to comparable anatomy and physiology of the ovine metatarsal and tarsal bones to those of humans. Approval for the surgeries performed on this animal was granted by the Colorado State University IACUC (Approval No. #1199). Surgery was performed under general anesthesia and aseptic conditions. The device was inserted through the calcaneus and advanced to span the calcaneus-tarsus-metatarsus complex and fixed using transverse screws. For the normal bone quality model, the first two devices, one dynamic and one static, were implanted successfully without complication in early 2021. The first animal with a dynamic device was sacrificed at a 4-month timepoint and the hindlimb harvested for further analysis. Following the first two successful implantations, four more animals were enrolled, two with a dynamic device and two with a static device in August 2021. Figures 28, 29, 30 further detail the surgical implantation with guidewire placement, joint reaming, trial sizer placement to determine device length, and final placement of the device.

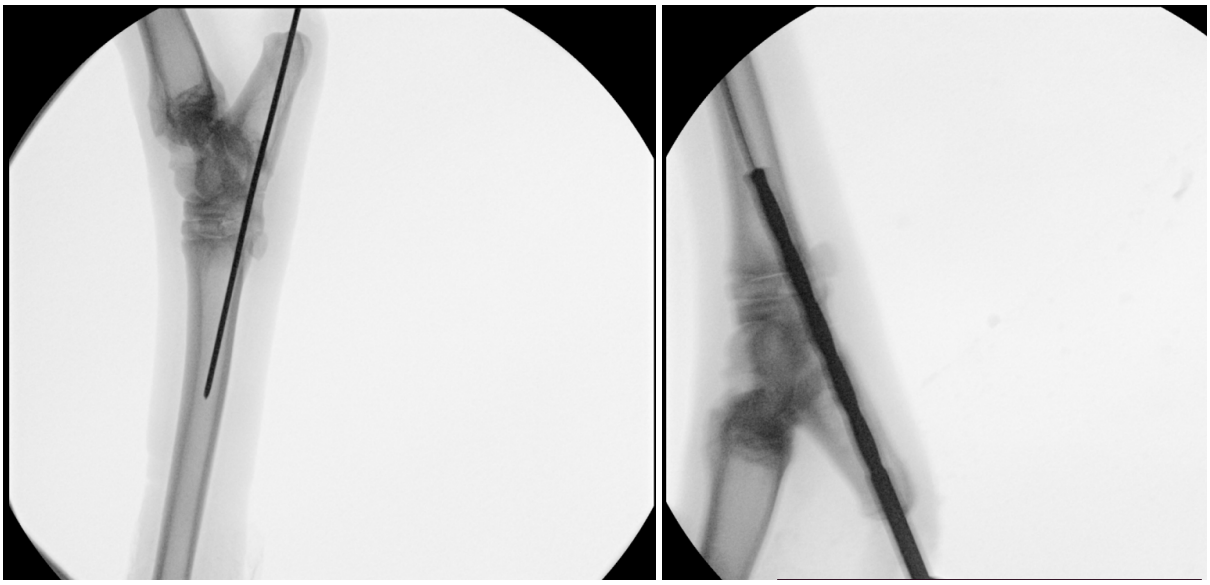

Figure 28. (left) Guidewire placement across the calcaneus-tarsal-metatarsal joint complex of the sheep hindlimb. (right) Reaming of joint prior to device placement.

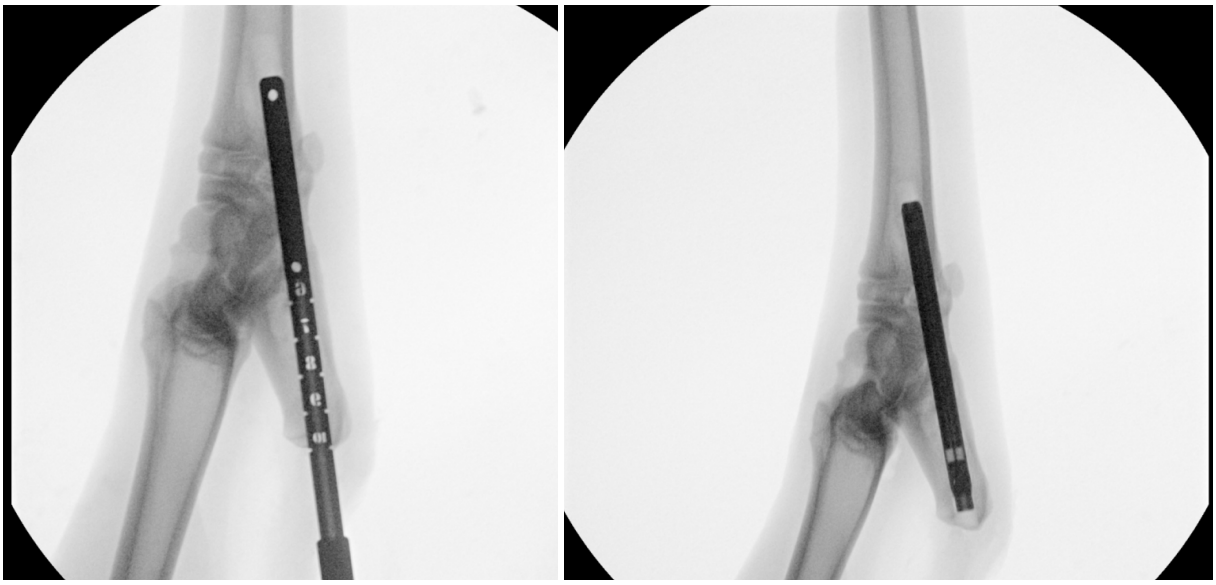

Figure 29. (left) Device length is determined by a trial sizer. (right) Placement of dynamic device.

Figure 30. (left) Radiograph of dynamic device post-operatively. (right) Radiograph of static device post-operatively.

Year 2 Accomplishments: From August 31, 2021 to July 7, 2022, all remaining animals in this Aim were enrolled following the above-described surgical procedures. There were a total of 32 animals in this Aim, 16 with a dynamic device and 16 with a static device. Surgical technique was refined by use of threaded guidewires to determine trajectory of the device. Figure 31 details the refined surgical technique. (1) An incision is made of the posterior aspect of the calcaneus. (2 and 3) A guidewire is passed from the calcaneus through the tarsals to the proximal metatarsal. (4) A 7.5 mm reamer is passed over the guidewire across the joints. (5) A sizing tool is used to determine the length of the device. A 7 mm x 100 mm device was used for all animals in both static and dynamic groups. (6) The sizing tool is removed, then the implant inserted to the proper depth, and manual compression applied. (7) The targeting frame is used to drill a lateral to medial hole through the bone and device. A headless cortical screw is inserted bicortically to lock the distal aspect of the device into the proximal metatarsal. (8) A headless cortical screw is inserted bicortically to lock the proximal aspect of the device into the calcaneus. (9 and 10) The insertion tool and targeting frame are removed from the implant, and the incision is closed in a routine manner. As of the end of year 2, 12 of 32 animals have reached their terminal endpoint.
Year 3 Accomplishments: As of the end of year 3, all 32 animals have reached their terminal endpoint. Upon successful conclusion of the animal study, including explants but prior to completion of biomechanical studies and histopathology, a study facility audit was successfully completed.

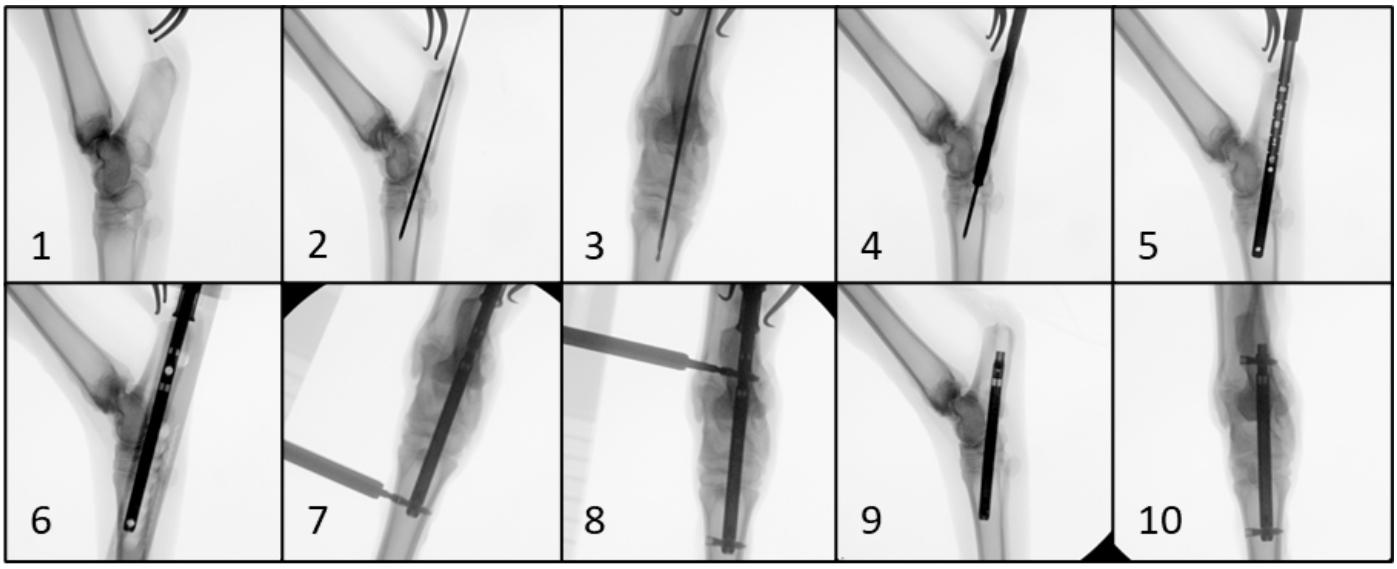

Figure 31. Refined surgical technique for device implantation surgery.

Training and Professional Development Opportunities: Nothing to Report
Dissemination of Results: Results were presented at the Orthopaedic Research Society Meeting in Tampa, FL, in February 2022, “Development of a Large Animal Model for Tarsal Fusion with Micro-CT Evaluation”.
Future Plan: No future plans. Surgeries complete. Terminal endpoints complete.
Status: Enrollment 100% complete. Terminal endpoints 100% complete.

Subtask 2-Radiographs
Year 1 Accomplishments: Serial radiographs were taken of each animal, in particular, the animals with dynamic devices because the decrease in the sliding element gap can be tracked to measure joint settling/bone resorption. Figure 32 shows the sequential movement of the sliding element within the outerbody over 4 months. Figure 33 shows a comparison of the post-operative distance, approximately 4 mm, to the 4-month distance, approximately 1 mm. Figure 34 shows the quantitative measurement of joint settling/bone resorption as determined by image analysis at each timepoint. Clinically, 3-5 mm of joint settling/bone resorption has been seen in patients with Charcot neuroarthropathy, thus 3 mm of joint settling/bone resorption in an ovine model represents the clinical scenario.

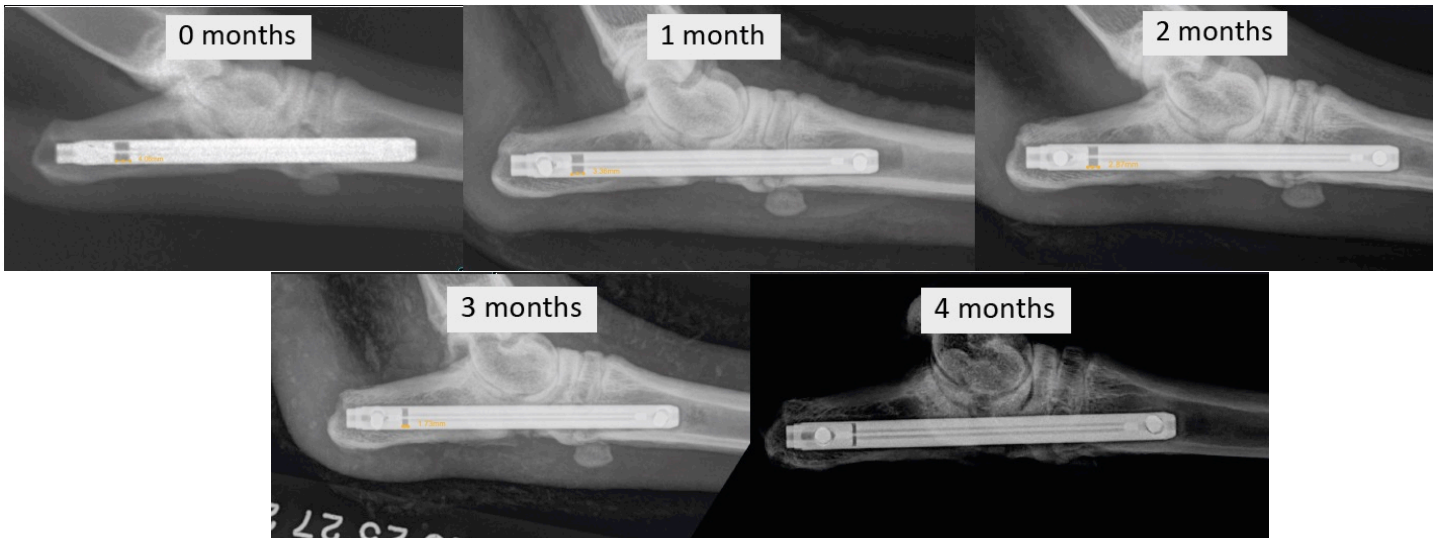

Figure 32. Serial radiographs for dynamic device.

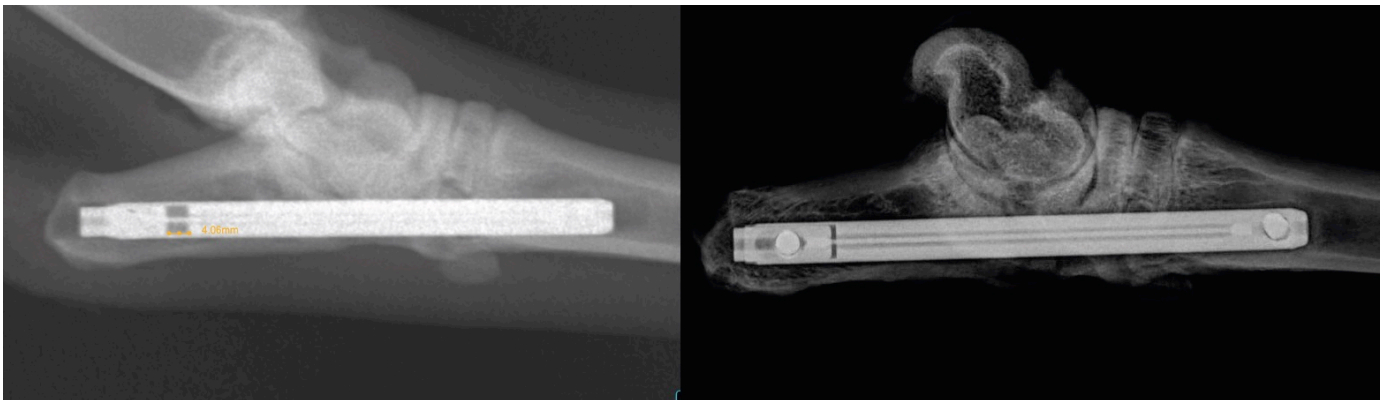

Figure 33. (left) Radiograph at post-op. (right) Radiograph after 4 months.

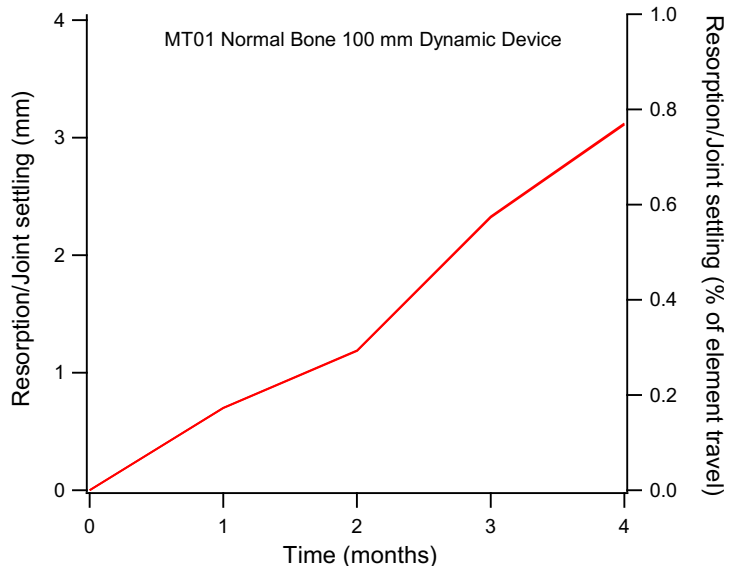

Figure 34. Quantitative evaluation of joint settling/bone resorption during post-operative healing.

Year 2 Accomplishments: Serial radiographs were taken and analyzed to track the movement of the nitinol element in the dynamic devices. Figure 35 shows the movement of the nitinol element as it adapts to bone resorption and joint settling. This is critical to verify that after 8 months of healing that the nitinol element starts to plateau and no longer move because this signifies that the bone has started to fuse and carry the load, instead of the device. It means that the arthrodesis has become mechanically stable. Also as important, the devices are not reaching 4 mm of bone resorption, which is the maximum amount possible for the dynamic devices, thus the dynamic devices continue to apply sustained dynamic compression during the entire course of healing. This is the literal proof that the device is working how it was designed.

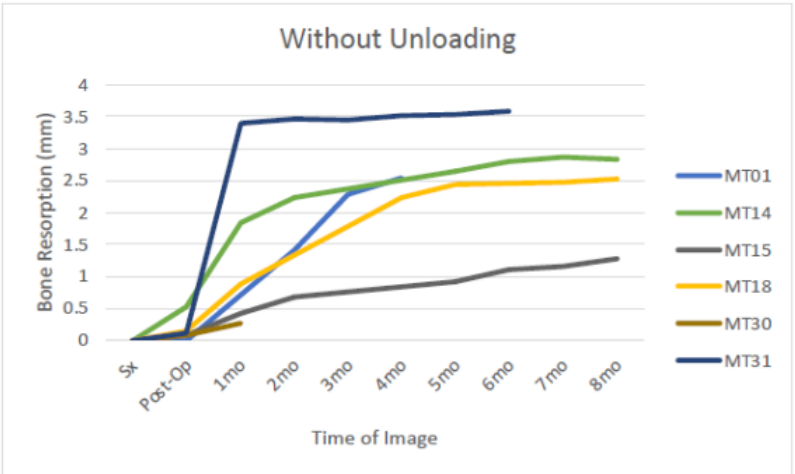

Figure 35. Bone resorption tracking of nitinol element in normal bone quality model.

Year 3 Accomplishments: Serial radiographs of the remaining animals were obtained, and nitinol element travel was quantified. Results were consistent with those observed in Year 2. Figure 36 shows the movement of the nitinol element as it adapts to bone resorption and joint settling. This is critical to verify that after 8 months of healing that the nitinol element starts to plateau and no longer moves, as that signifies that the bone has started to fuse and carry the load (instead of the device). In short, it is indicative of the arthrodesis becoming mechanically stable (a point further validated by mechanical testing results). Of note, these data illustrate that the dynamic devices continue to apply sustained dynamic compression during the entire course of healing as they have not reached their maximum travel (4 mm, indicated by red line on Figure 36). This serves to prove the intended/designed mechanism of action of this device is operating correctly in a live animal model.

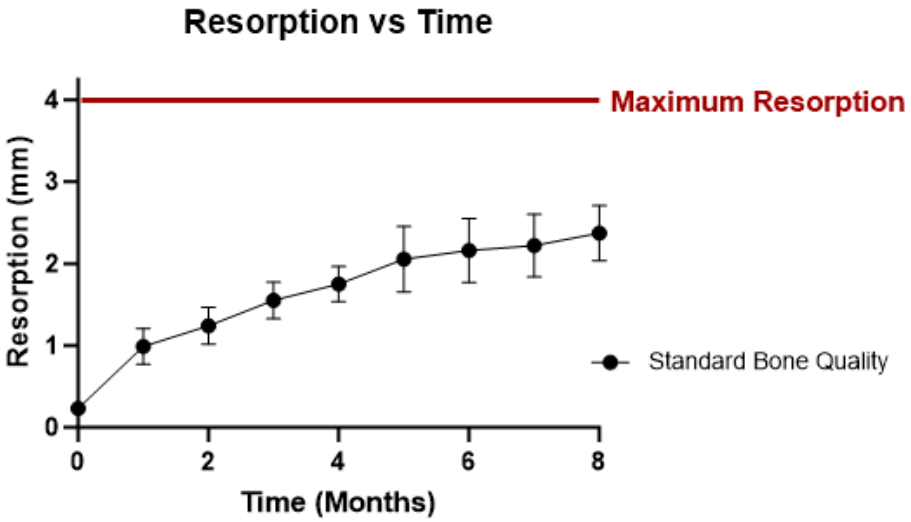

Figure 36. Bone resorption tracking of nitinol element in normal / standard bone quality model.

Training and Professional Development Opportunities: Nothing to Report
Dissemination of Results: Initial results were presented at the Orthopaedic Research Society Meeting in Tampa, FL, in February 2022, “Development of a Large Animal Model for Tarsal Fusion with Micro-CT Evaluation”. Additional results were presented at the Orthopaedic Research Society Meeting in Dallas, TX, in February 2023, “Tracking Bone Resorption with Sustained Dynamic Compression in a Novel Large Animal Model of Tarsal Fusion”.
Future Plan: None. All radiographs obtained and element travel quantified.
Status: 100% Complete.

Subtask 3-Mechanical Evaluation
Year 1 Accomplishments: Mechanical testing from the first animal has been completed by using a nondestructive 4-point bending test (Figure 37). Five conditioning cycles were used to load the construct to 1000 N at a rate of 1 mm/s. The data was taken from the last loading cycle. The stiffness was determined to be 1459 N/mm.

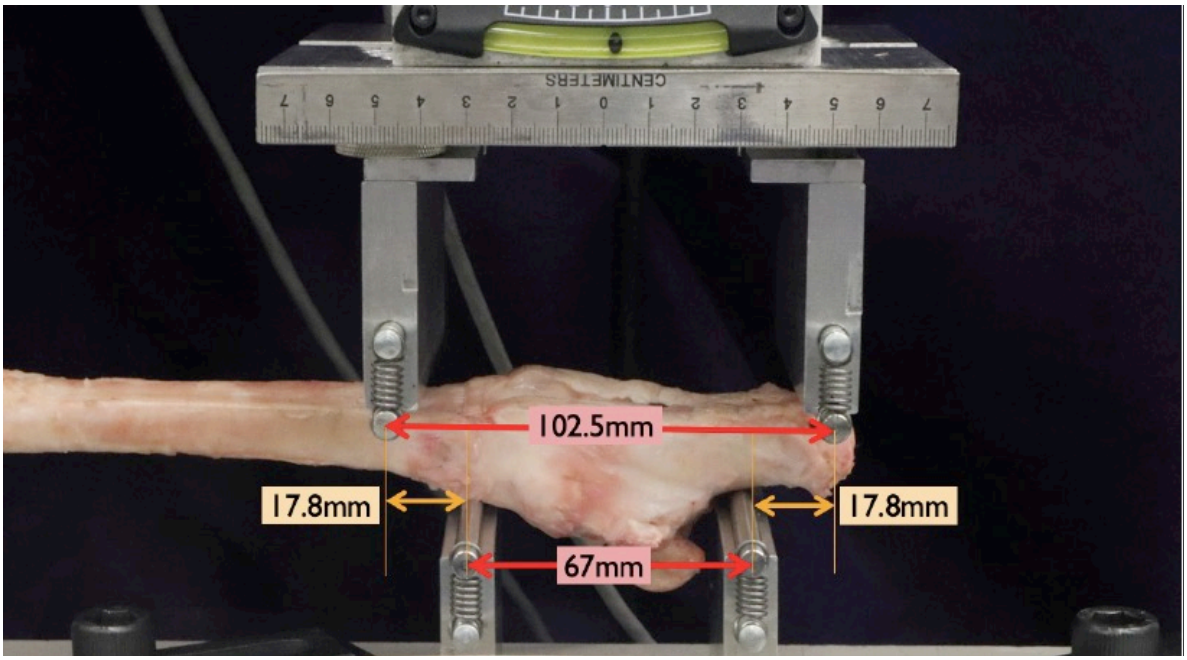

Figure 37. 4-point bend test setup for ovine hindlimbs.

Year 2 Accomplishments: As animals reached their endpoint, hindlimbs were harvested and prepared for biomechanical testing. Using previous methods, a nondestructive 4-point bending test was used to load the construct to 1000 N at a rate of 1 mm/s. The data was taken from the last loading cycle after five conditioning cycles. The raw data for the static and dynamic groups for 4-point bending test is shown in Figure 38. The average stiffness from the load-displacement data is shown in Figure 39. The contralateral limb has a stiffness of 295 N/mm as the limb is more flexible because it has not undergone fusion. The data herein represents the 8-month timepoint for both static and dynamic devices. It is important to note that the fusion device is present in the specimen when this test is taking place, thus a highly rigid construct is expected. These are initial results that are not the full sample size for each group at each respective timepoints of 4 months and 8 months. The average stiffness was 969±291 N/mm for the static group and 1104±193 N/mm for the dynamic group when taking the slope between 400-600 N. Without the remaining dataset, conclusions should not yet be made. However, it is clear that the fusion surgery significantly increases the stiffness of the construct compared to the contralateral unoperated hindlimb.

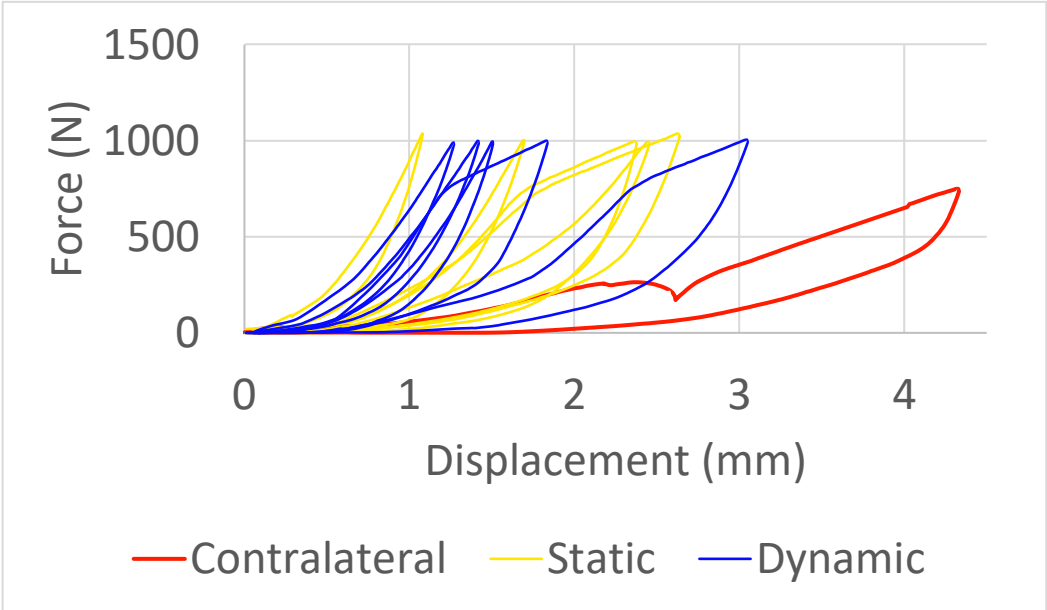

Figure 38. Load-displacement data from 4-point bending test.

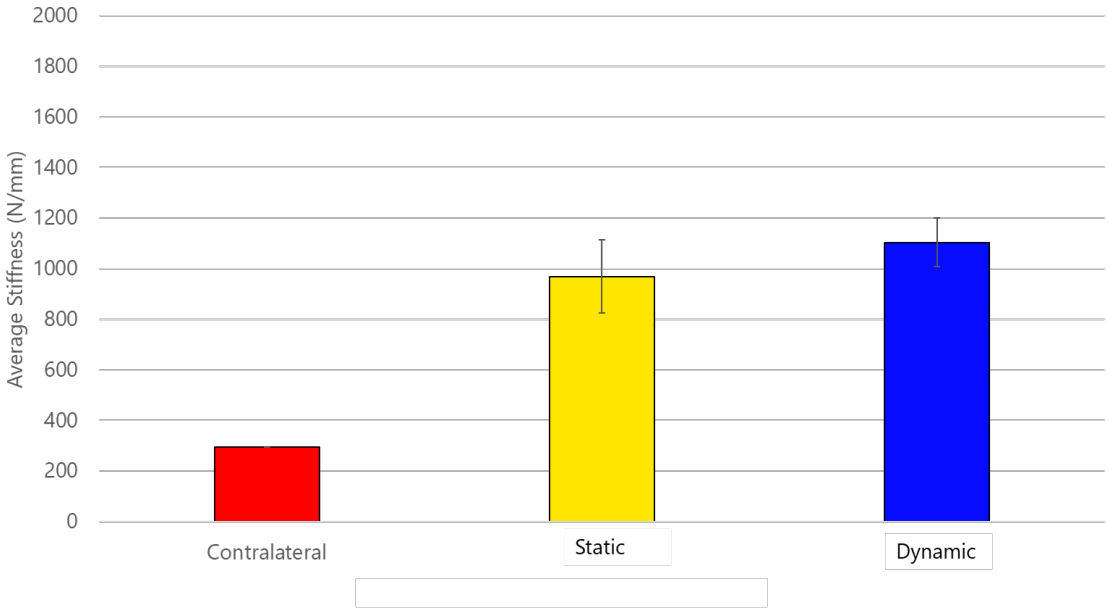

Figure 39. Average stiffness from 4-point bending test.

Year 3 Accomplishments: All animals have reached their terminal endpoint, and all fusion constructs (static and dynamic) have undergone 4-point biomechanical testing using the same methods described previously (loading to 1,000 N; 1 mm/s; inner span = 67 mm; outer span = 102.5 mm). These data (Figure 40) illustrate (1) the significant decrease in construct stiffness in samples treated with a static device and (2) the maintained construct stiffness in samples treated with a dynamic device (which was significantly increased as compared to 8-month static group). These data illustrate the construct level benefits of maintaining sustained dynamic compression over the entire fusion period.

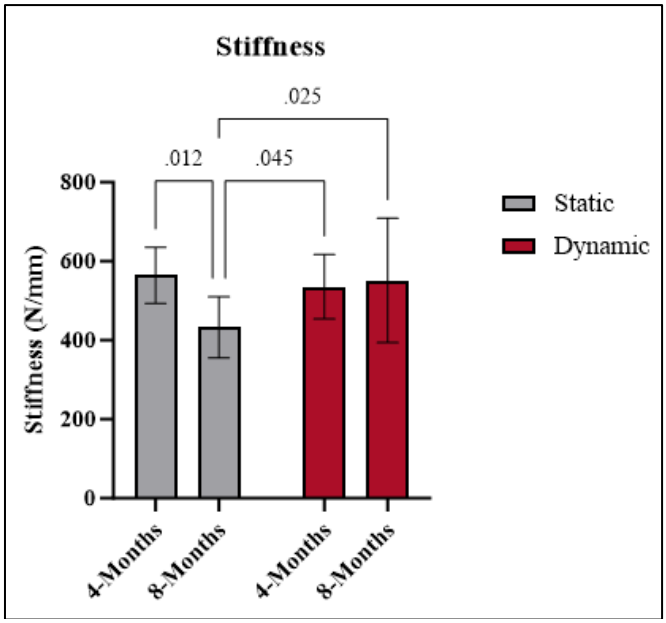

Figure 40. Four-point bending construct stiffness of fusion constructs with static and dynamic fixation devices at both 4- and 8-months post-op.

Training and Professional Development Opportunities: Nothing to Report
Dissemination of Results: These data have been presented at the MHSRS 2023 meeting in Orlando, FL.
Future Plan: None.
Status: 100% Complete.

Subtask 4-Micro-CT

Year 1 Accomplishments: Micro-computed tomography (micro-CT) scans were performed on both the treated and contralateral hock joints at a resolution of 37 μm (Scanco μCT 80, Scanco Medical AG, Bruttisellen, Switzerland). The device was carefully removed from the treated joint before scanning to eliminate inaccuracies attributable to radiographic artifact. The region of interest of each specimen was centered over the interfaces of the tarsal bones (Figure 39) and each region was evaluated for bone volume (BV) and mean density of the bone volume (MDBV) using automatic segmentation techniques with thresholds to a range of 250 and 450 mgHA/ccm. To further minimize error due to automatic segmentation practices, the contralateral limb was evaluated using the same parameters to establish a baseline. New bone formation of the treated limb was calculated by the difference in bone volume of the treated and contralateral limbs. The volume of immature bone was 26.3% higher within the defined ROI in the treated limb than in the untreated limb. Bone formation was observed primarily around the outside of the joint with visible evidence of preliminary bridging across some of the intertarsal joint capsules (Figure 41). The volume of bone reported between the threshold limits was measured as 5,740 mm^3 in the treated joint complex compared to 4,545 mm^3 in the contralateral. The mean density of regions of immature bone was 328 mgHA/ccm and 301 mgHA/ccm in the treated and contralateral limbs, respectively.

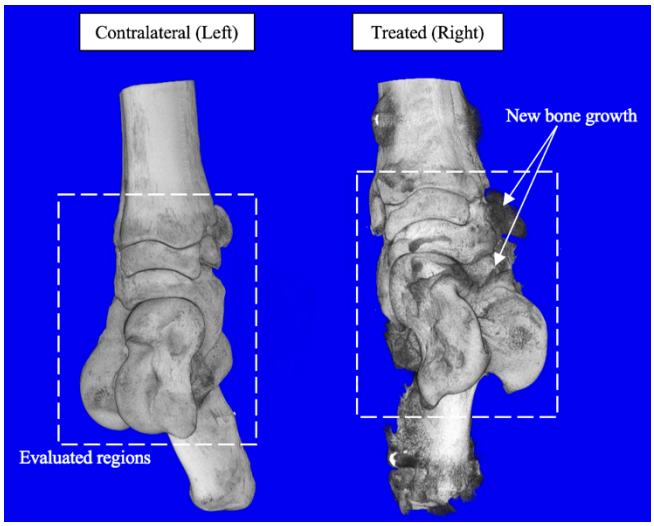

Figure 41. Micro-CT of ovine hock joints.

Year 2 Accomplishments: 20 samples from 10 animals have been scanned via micro-CT. Another 12 samples from 6 animals have been prepared to be scanned. Full reconstructions of 6 samples from 3 animals have been fully processed. Figure 42 shows the micro-CT from a static device. New bone formation of the treated limb was calculated by the difference in bone volume of the treated and contralateral limbs. The volume of immature bone was 2.9% higher within the defined ROI in the treated limb than in the untreated limb. Limited bone formation was observed near the outside of the joint (Figure 40). The volume of bone reported between the threshold limits was measured as 4,215 mm^3 in the treated joint complex compared to 4,098 mm^3 in the contralateral. The mean density of regions of immature bone was 321 mgHA/ccm and 287 mgHA/ccm in the treated and contralateral limbs, respectively.

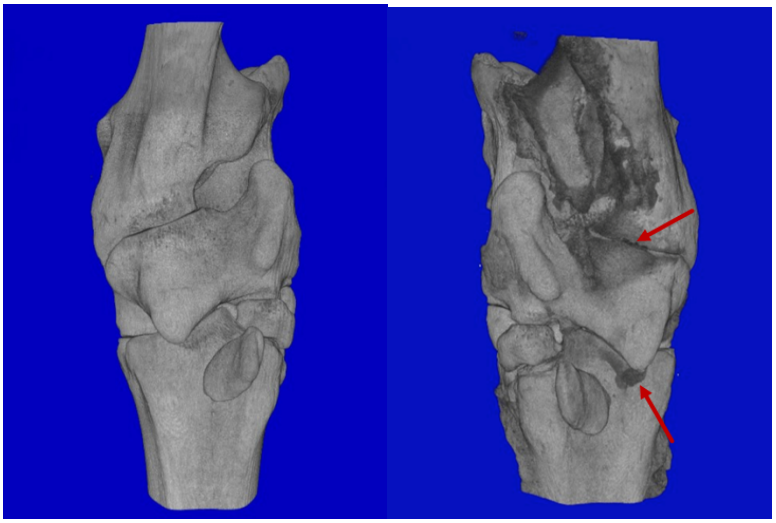

Figure 42. (left) Contralateral (right) Fused ovine hock joint.

Year 3 Accomplishments: All samples have undergone micro-CT scanning at 37-micron resolution. Micro-CT analysis is currently ongoing; 31 out of 32 samples have been analyzed to quantify bone volume, bone volume fraction, mean density bone volume, and mean density total volume. The region of analysis for all samples captures the intrajoint space within the three-bone fusion segment. Figures depicting these outcome parameters for both device types at both time points are included below (Figure 43). The Dynamic group continued to increase bone volume through the 8-month time point; whereas the static group exhibited nearly equivalent bone volumes at the 4- and 8-month time points. No significant differences were noted in the other micro-CT outcome parameters (i.e., bone volume fraction, mean density bone volume, and mean density total volume).

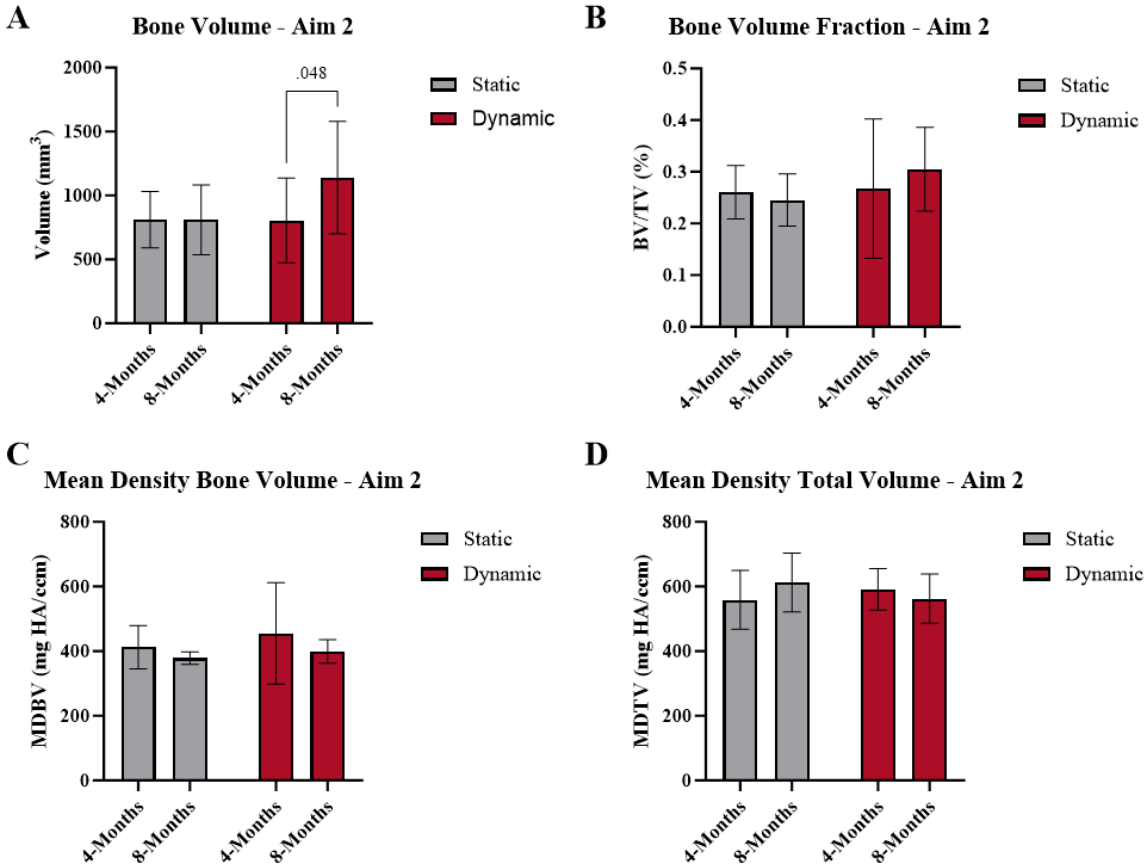

Figure 43. Aim 2 micro-CT results. A) Bone volume. B) Bone volume fraction. C) Mean density bone volume. D) Mean density total volume.

Training and Professional Development Opportunities: Nothing to Report.

Dissemination of Results: Initial results were presented at the Orthopaedic Research Society Meeting in Tampa, FL, in February 2022, “Development of a Large Animal Model for Tarsal Fusion with Micro-CT Evaluation”.
Future Plan: Micro-CT analysis will occur for all remaining animals during the study period.
Status: 97% Complete. Analysis needs to be completed on the one remaining sample prior to completion of this dataset. This is expected to be completed by end of 2023.

Subtask 5-Histological Evaluation
Year 1 Accomplishments: Nothing to Report.
Year 2 Accomplishments: Histological processing has started. 12 samples from 6 animals have been cut into gross slabs and infiltrated with 70% ethanol. After infiltration, embedding will occur into paraffin or acrylosin, then histological analysis will be performed.
Year 3 Accomplishments: All samples have been cut into gross slabs (segmented to region of interest) and infiltrated with 70% ethanol. After infiltration, samples were/will be embedded in acrylosin, sectioned using a diamond fine kerf precision band saw, then ground to final slide thickness of 50-70 microns. Unstained histology slides have been generated for 10 out of 32 samples. These unstained slides have been imaged using fluorescent slide imaging techniques on an automated slide scanner to enable dynamic histomorphometry analysis. The remaining histology slides are expected to be completed by January 2024. Upon completion of all histology slides and following fluorescent imaging of all unstained slides for dynamic histomorphometry analysis, all slides will be stained with Sanderson bone stain followed with a van gieson counterstain. These stained slides will be imaged using brightfield microscopy techniques and will undergo static histomorphometry analysis to quantify tissue components (e.g., percent bone area, percent fibrous tissue area, percent implant, percent empty space). Stained histology slides will be analyzed by the study histopathologist using ISO 10993-6 standards for biological evaluation of medical devices as well as relevant fusion characteristics. The histopathology analysis is expected to be complete prior to June 2024.

Training and Professional Development Opportunities: Nothing to Report
Dissemination of Results: Nothing to Report.
Future Plan: Histological processing will occur for all specimens collected during the study period by January 2024. Dynamic histomorphometry, static histomorphometry, and histopathology analyses are expected to be completed by June 2024.
Status: Histology slide generation 31% complete. Static histomorphometry, dynamic histomorphometry, and histopathology analyses 0% complete.

*3.2.2 **Major Task 3:** Validate the prototype device’s ability to apply dynamic compression in vivo using an ovine hindlimb fusion model with low bone quality.*

Subtask 1-Partial Unload Surgery
Year 1 Accomplishments: The first partial unload surgery took place in the second quarter of 2021 following CSU IACUC 1199 to attach an external fixator across the hock joint of the ovine hindlimb for a period of 4 weeks to decrease the bone quality. A representative image of the external fixator is shown in Figure 44. Additional animals were enrolled at the beginning of August 2021 with external fixators for 4 weeks.

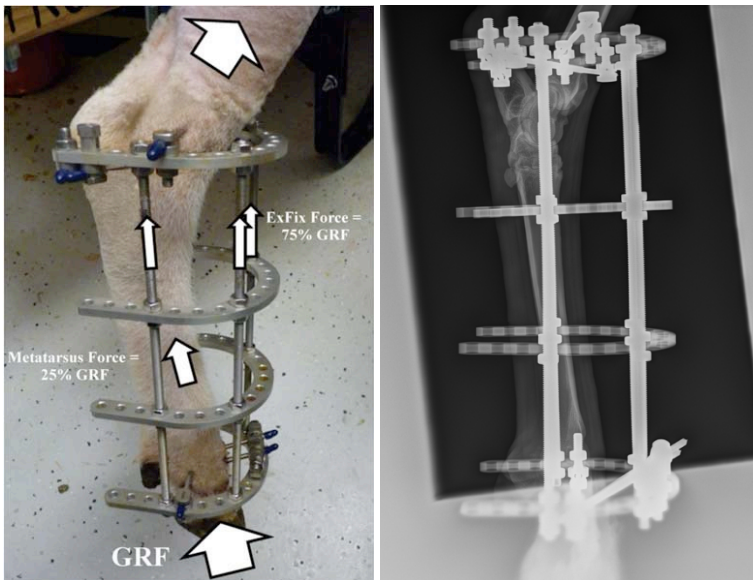

Figure 44. External fixator placement on ovine hindlimb.

Year 2 Accomplishments: From January 10, 2022 to August 10, 2022, all remaining animals in this Aim were enrolled following the above-described surgical procedures from Year 1 (Figure 45). There are a total of 32 animals in this Aim, 16 with a dynamic device and 16 with a static device.

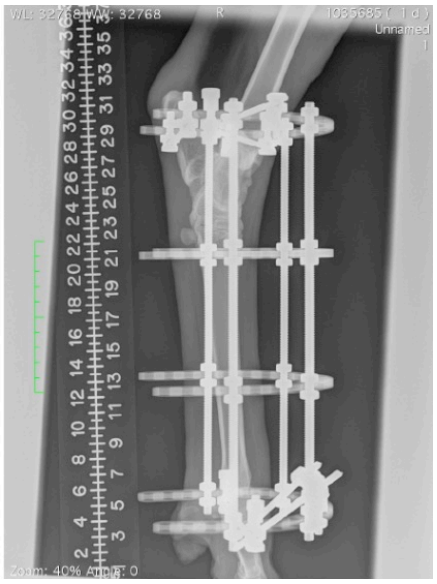
Figure 45. Radiograph of ex-fix placed across the hock joint to lower bone quality.

Training and Professional Development Opportunities: Nothing to Report
Dissemination of Results: Nothing to Report
Future Plan: No future plans. Ex-fix surgeries complete.
Status: 100% Enrollment. Task complete.

Subtask 2-Fusion Surgery
Year 1 Accomplishments: The first animal with lower bone quality successfully underwent device implantation following CSU IACUC 1199. The same procedures and protocols were followed for device implantation as Major Task 2 Subtask 1. A dynamic device was implanted in the first animal and post-op radiograph is shown in Figure 46.

Figure 46. Radiograph post-op of dynamic device in ovine hindlimb after removal of external fixator.

Year 2 Accomplishments: Between February 8, 2022, and July 26, 2022, a total of 30 animals had fusion surgery after removal of external fixator. The same surgical procedures were followed as in Major Task 2 Subtask 1.
Year 3 Accomplishments: As of the end of Year 3, all 32 animals have reached their terminal endpoint including successful completion of bone quality depletion and subsequent fusion surgery.
Training and Professional Development Opportunities: Nothing to Report
Dissemination of Results: Nothing to Report
Future Plan: None. All fusion surgeries completed.
Status: 100% Complete.

Subtask 3-Radiographs
Year 1 Accomplishments: As in Major Task 2 Subtask 2, serial radiographs are taken of each animal, especially the animals with dynamic devices because the decrease in the sliding element gap can be tracked to measure joint settling/bone resorption. The two-month timepoint radiograph is shown in Figure 47 for the first animal with low bone quality.

Figure 47. Two-month radiograph for animal with low bone quality and dynamic device.

Year 2 Accomplishments: Serial radiographs were taken and analyzed to track the movement of the nitinol element in the dynamic devices. Figure 48 shows the movement of the nitinol element as it adapts to bone resorption and joint settling. This is critical to verify that near 6 months of healing that the nitinol element starts to plateau and no longer move because this signifies that the bone has started to fuse and carry the load, instead of the device. It means that the arthrodesis has become mechanically stable. Also as important, the devices are

not reaching 4 mm of bone resorption, which is the maximum amount possible for the dynamic devices, thus the dynamic devices continue to apply sustained dynamic compression during the entire course of healing. This is the literal proof that the device is working how it was designed.

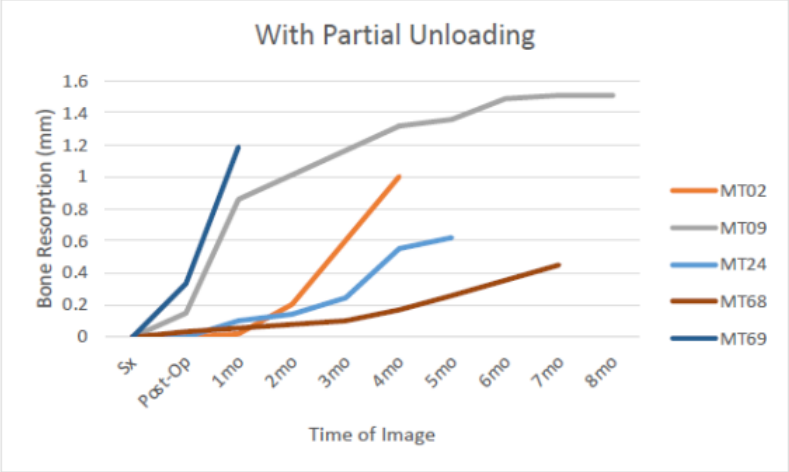

Figure 48. Bone resorption tracking of nitinol element in low quality bone model.

Year 3 Accomplishments: Serial radiographs of the remaining animals were obtained, and nitinol element travel was quantified. Results were consistent with those observed in Year 2. Figure 49 shows the movement of the nitinol element as it adapts to bone resorption and joint settling. This is critical to verify that after 8 months of healing that the nitinol element starts to plateau and no longer moves, as that signifies that the bone has started to fuse and carry the load (instead of the device). In short, it is indicative of the arthrodesis becoming mechanically stable (a point further validated by mechanical testing results). Of note, these data illustrate that the dynamic devices continue to apply sustained dynamic compression during the entire course of healing as they have not reached their maximum travel (4 mm, indicated by red line on Figure 49). This serves to prove the intended/designed mechanism of action of this device is operating correctly in a live animal model.

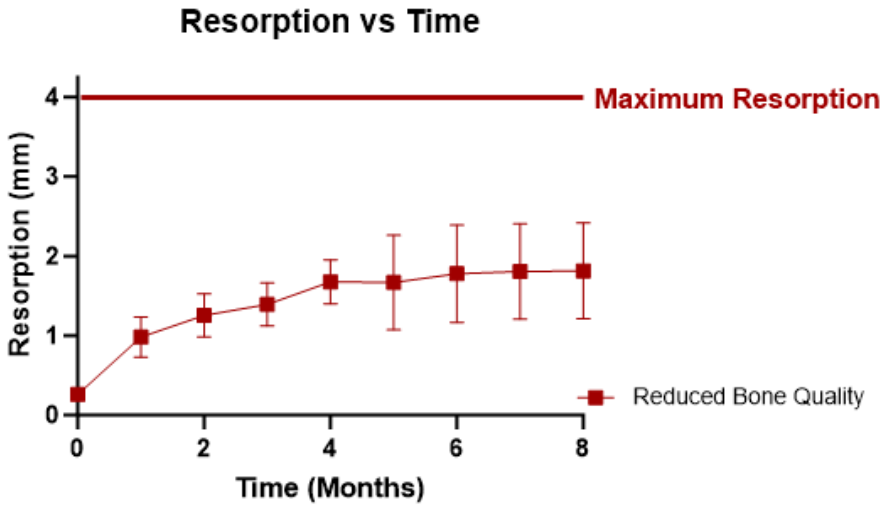

Figure 49. Bone resorption tracking of nitinol element in low quality bone model.

Training and Professional Development Opportunities: Nothing to Report
Dissemination of Results: An abstract was submitted to the 2023 Military Health System Research Symposium (MHSRS), “Sustained Dynamic Compression Device Provides Continuous Compression in the Setting of Bone Resorption Following Arthrodesis in an Ovine Model.” The abstract was accepted for poster presentation, which occurred in August 2023, in Orlando, FL.
Future Plans: None. All radiographs obtained and element travel quantified.
Status: 100% Complete.

Subtask 4-Mechanical Evaluation

Year 1 Accomplishments: Nothing to Report
Year 2 Accomplishments: As animals reached their endpoint, hindlimbs were harvested and prepared for biomechanical testing. Using previous methods, a nondestructive 4-point bending test was used to load the construct to 1000 N at a rate of 1 mm/s. The data was taken from the last loading cycle after five conditioning cycles. The raw data for the static and dynamic groups for 4-point bending test is shown in Figure 50. The average stiffness from the load-displacement data is shown in Figure 51. The contralateral limb has a stiffness of 295 N/mm as the limb is more flexible because it has not undergone fusion. The data herein represents the 8-month timepoint for both static and dynamic devices. It is important to note that the fusion device is present in the specimen when this test is taking place, thus a highly rigid construct is expected. These are initial results that are not the full sample size for each group at each respective timepoint of 4 months and 8 months. The average stiffness was 1185 ± 112 N/mm for the static group and 1228 ± 237 N/mm for the dynamic group when taking the slope between 400-600 N. Without the remaining dataset, conclusions should not yet be made. However, it is clear that the fusion surgery significantly increases the stiffness of the construct compared to the contralateral unoperated hindlimb.

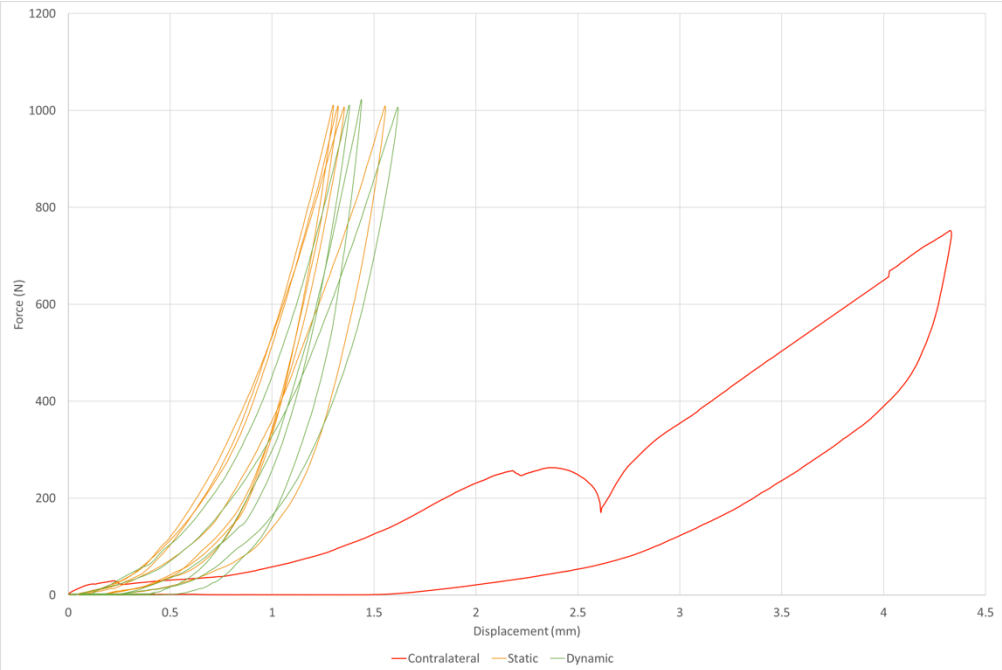

Figure 50. Load-displacement data from 4-point bending test.

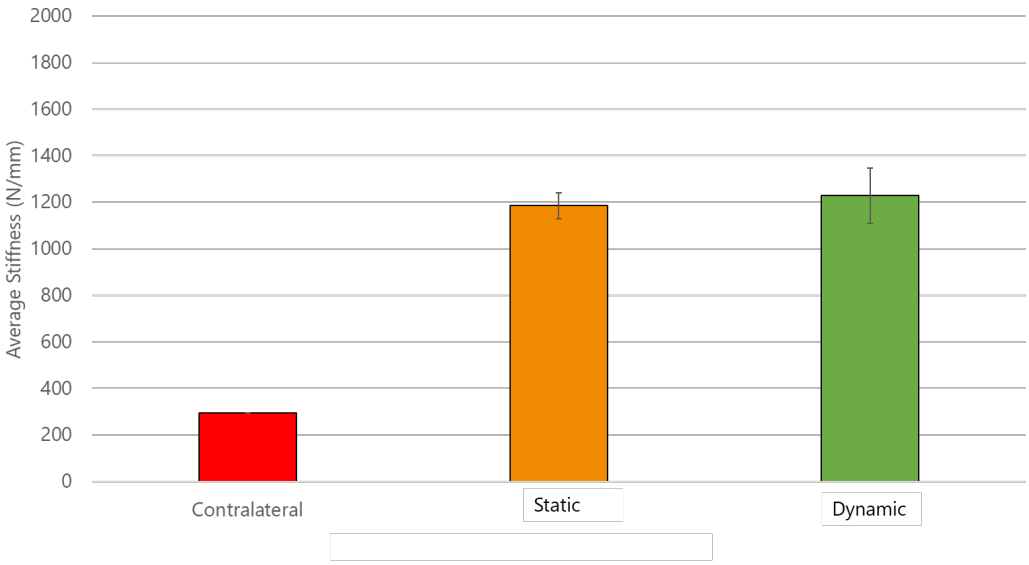

Figure 51. Average stiffness from 4-point bending test.

Year 3 Accomplishments: All animals have reached their terminal endpoint, and all fusion constructs (static and dynamic) have undergone 4-point biomechanical testing using the same methods described previously (loading

to 1,000 N; 1 mm/s; inner span = 67 mm; outer span = 102.5 mm). No significant differences were noted in stiffness between the devices or timepoints (Figure 52). These data illustrate that fusion with the dynamic device generates a construct of equivalent rigidity as compared to the static device. As the dynamic device is designed to apply axial compression across the fusion construct, it is not expected to generate a construct that would be stiffer in bending.

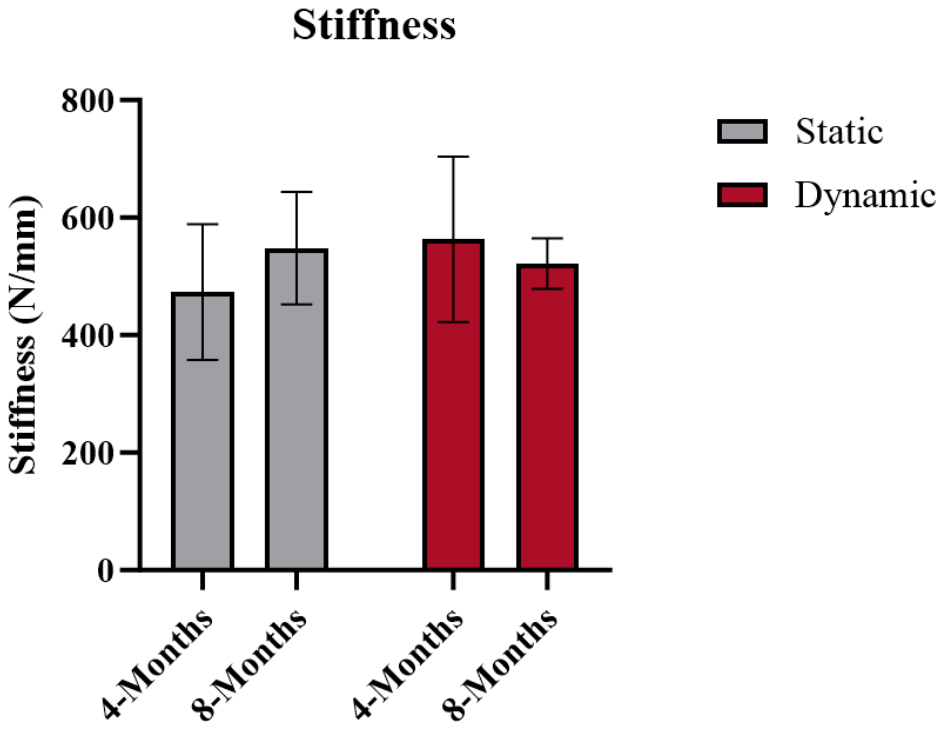

Figure 52. Stiffness of the static and dynamic samples across the 4- and 8-month time points. No significant differences were noted in stiffness between treatment groups or time points.

Training and Professional Development Opportunities: Nothing to Report
Dissemination of Results: These results have been presented at the 2023 MHSRS conference in August 2023 in Orlando, FL.
Future Plan: None.
Status: 100% Complete.

Subtask 5-Micro-CT
Year 1 Accomplishments: Nothing to Report
Year 2 Accomplishments: 20 samples from 10 animals have been scanned via micro-CT. Another 16 samples from 8 animals have been prepared to be scanned. Full reconstructions of 4 samples from 2 animals have been fully processed. No conclusions can be drawn currently as full data sets have not been processed. Figure 53 shows the micro-CT from a dynamic device at 4-month timepoint. New bone formation of the treated limb was calculated by the difference in bone volume of the treated and contralateral limbs. The volume of immature bone was 9.1% higher within the defined ROI in the treated limb than in the untreated limb. Bone formation was observed near the outside of the joint and the beginning of bone bridging across some of the joints occurred (Figure 48). The volume of bone reported between the threshold limits was measured as 5,182 mm^3 in the treated joint complex compared to 4,750 mm^3 in the contralateral. The mean density of regions of immature bone was 314 mgHA/ccm and 304 mgHA/ccm in the treated and contralateral limbs, respectively. Additionally, micro-CT was used to verify that the unloading procedure had decreased the bone quality in this animal group (Figure 54). Control animals from Major Task 2 showed a 3.1% change in trabecular thickness and a 1.2% change in trabecular spacing. Animals that underwent the unloading procedure showed a 21.1% decrease in trabecular thickness and a 34.4% increase in trabecular spacing, thus their bone quality decreased with thinner struts and larger pores. This serves as verification that the unloading procedure is reducing the bone quality.

Figure 53. (left) Contralateral, (right) Fused ovine hock joint microCT scan.

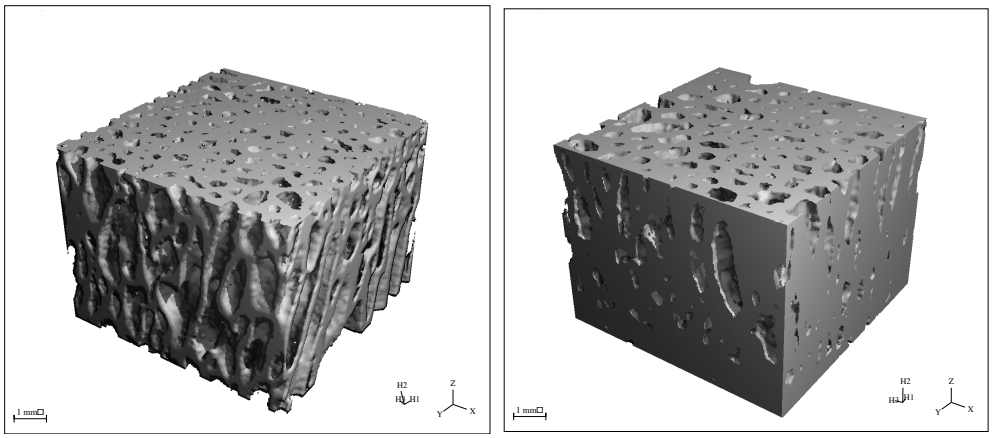

Figure 54. (left) Micro-CT from animal that underwent unloading procedure with decreased bone quality. (right) Micro-CT from animal that has normal bone quality.

Year 3 Accomplishments: All samples have undergone micro-CT scanning at 37-micron resolution. Micro-CT analysis is currently ongoing; 28 out of 32 samples have been analyzed to quantify bone volume, bone volume fraction, mean density bone volume, and mean density total volume. The region of analysis for all samples captures the intrajoint space within the three-bone fusion segment. Figures depicting these outcome parameters for both device types at both timepoints are included below (Figure 55). No significant differences were noted in any micro-CT outcome parameters between the device types or timepoints.

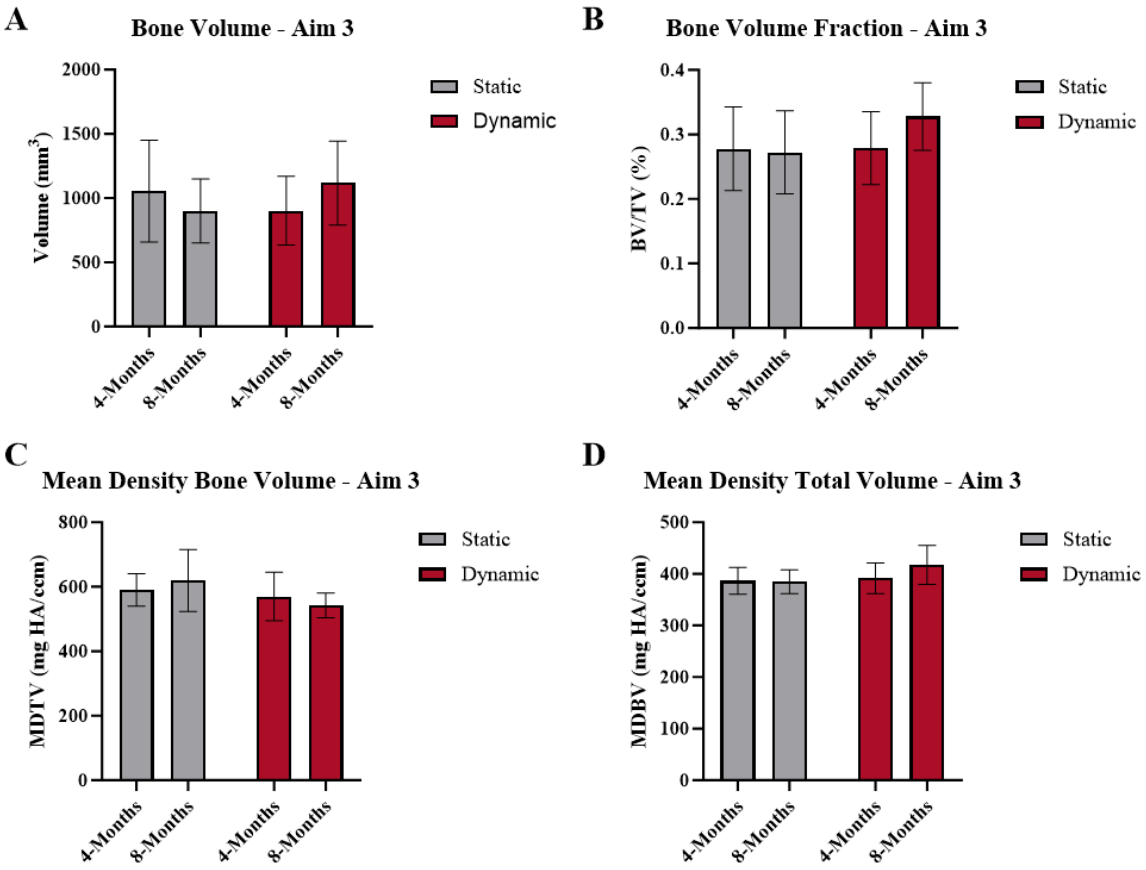

Figure 55. Aim 3 micro-CT results. A) Bone volume. B) Bone volume fraction. C) Mean density bone volume. D) Mean density total volume.

Training and Professional Development Opportunities: Nothing to Report.
Dissemination of Results: Initial results were presented at the Orthopaedic Research Society Meeting in Tampa, FL, in February 2022, “Development of a Large Animal Model for Tarsal Fusion with Micro-CT Evaluation”.
Future Plan: Micro-computed tomography analysis will occur for all remaining animals during the study period.
Status: 97% Complete. Analysis needs to be completed on the four remaining samples prior to completion of this dataset. This is expected to be completed by end of 2023.

Subtask 6-Histological Evaluation
Year 1 Accomplishments: Nothing to Report
Year 2 Accomplishments: Histological processing has started. 10 samples from 5 animals have been cut into gross slabs and infiltrated with 70% ethanol. After infiltration, embedding will occur into paraffin or acrylosin, then histological analysis will be performed.
Year 3 Accomplishments: All samples have been cut into gross slabs (segmented to region of interest) and infiltrated with 70% ethanol. After infiltration, samples were/will be embedded in acrylosin, sectioned using a diamond fine kerf precision band saw, then ground to final slide thickness of 50-70 microns. Unstained histology slides have been generated for 11 out of 32 samples. These unstained slides have been imaged using fluorescent slide imaging techniques on an automated slide scanner to enable dynamic histomorphometry analysis. The remaining histology slides are expected to be completed by January 2024. Upon completion of all histology slides and following fluorescent imaging of all unstained slides for dynamic histomorphometry analysis, all slides will be stained with Sanderson bone stain followed with a van gieson counterstain. These stained slides will be imaged using brightfield microscopy techniques and will undergo static histomorphometry analysis to quantify tissue components (e.g., percent bone area, percent fibrous tissue area, percent implant, percent empty space). Stained histology slides will be analyzed by the study histopathologist using ISO 10993-6 standards for biological evaluation of medical devices as well as relevant fusion characteristics. The histopathology analysis is expected to be complete prior to June 2024.

Training and Professional Development Opportunities: Nothing to Report
Dissemination of Results: Nothing to Report.

Future Plan: Histological processing will occur for all specimens collected during the study period by January 2024. Dynamic histomorphometry, static histomorphometry, and histopathology analyses are expected to be completed by June 2024. A second facility audit will be completed once all biomechanical and histopathology work is concluded.
Status: Histology slide generation 34% complete. Static histomorphometry, dynamic histomorphometry, and histopathology analyses 0% complete.

4. Impact

4.1 Impact on the development of the principal discipline

Project results to date present evidence of an orthopedic medical device with mechanical properties superior to current competitor devices that is also capable of sustaining compressive loads in the face of bone resorption or other factors that would be associated with gapping between fusing bones. This gapping often occurs in at-risk patient populations such as diabetics with Charcot neuroarthropathy. The sustained compression demonstrated and the ability to adapt to bone resorption by the project device in both mechanical testing and large animal model will add to the existing list of clinical and pre-clinical evidence supporting a shift in the orthopedic foot and ankle surgery discipline from static devices incapable of post-day of surgery change to dynamic adaptive compression devices that can contribute to fusion throughout the extended healing process.

4.2 Impact on other disciplines

The fundamental mechanobiological principles of joint fusion via sustained dynamic compression hold across multiple joints, whether in the foot and ankle or beyond, such as upper extremities. As such, other orthopedic surgical disciplines could show improved clinical outcomes via adoption of sustained dynamic compression devices similar to that developed in this project.

4.3 Impact on technology transfer

While no official transfer has occurred to date in the project, a portion of the study results to date were submitted and accepted for presentation at the 2021, 2022, and 2023 Military Health System Research Symposium, such that the study results to date would be shared with the military medical community. Additionally, results were shared at the 2022 and 2023 Orthopaedic Research Society meetings. Future project activities include regulatory submission to the FDA so that the device can be used clinically, and in particular used in at-risk patients, especially the Veteran population, who are not being adequately treated using existing static internal fixation technology. Project results to date suggest that the prototype device will be found to be substantially equivalent to competitor devices already cleared by the FDA.

4.4 Impact on society beyond science and technology

While there is nothing to report for the current period, there is a likely future impact due to the project and its results. Current product biomechanical testing data indicate that the study device is capable of sustaining compression in simulated joint fusion. Other MedShape joint fusion internal fixation devices providing sustained compression have already been granted their own unique ICD-10-PCS code by the US Centers for Medicare and Medicaid Services (DynaNail, DynaNail Mini, DynaNail Hybrid, DynaNail Helix, DynaClip, and DynaClip Forte). It is likely that the subject prototype device will also be eligible for addition in this unique coding set. CMS granted the code based upon data showing novelty and clinical superiority of sustained compression fixation devices to standard static fixation devices. This superiority has led to improved human health and capabilities in recipient patients, thus allowing them earlier and greater potential return to work where they can contribute to the workforce and help to drive the US economy, as well as engage in social activities requiring mobility and activity.

5. Changes/Problems

5.1 Changes in approach and reasons for change

Nothing to Report

5.2 Actual or anticipated problems or delays and actions or plans to resolve them

Histological preparation and analysis of samples from the large animal model has taken longer than initially anticipated, as these tasks are rigorous and time-consuming. As such, a no-cost project extension was sought and granted to focus on completing this work. The subaward facility has dedicated additional resources (staff) to ensure the aforementioned timelines are maintained.

5.3 Changes that had a significant impact on expenditures
Nothing to Report

5.4 Significant changes in use or care of vertebrate animals
Nothing to Report

6. Products
6.1 Publications, conference papers, and presentations
Two abstracts were submitted to the 2022 Orthopaedic Research Society meeting, “Development of a Large Animal Model for Tarsal Fusion with Micro-CT Evaluation”, and “Biomechanical Comparison in Synthetic Bone of Dynamic Versus Static Intramedullary Fixation Devices for Midfoot Arthrodesis”. The abstracts were accepted for poster presentation, which occurred in February 2022. An abstract was submitted to the 2022 Military Health System Research Symposium, “In Vitro and In Vivo Performance of a Sustained Dynamic Compression Fusion Device for Lower Extremity Salvage of the Diabetic Foot”. The abstract was accepted for a poster presentation, which occurred in August 2022. One abstract was submitted to the 2023 Orthopaedic Research Society meeting, “Tracking Bone Resorption With Sustained Dynamic Compression In A Novel Large Animal Model Of Tarsal Fusion.” The abstract was accepted for poster presentation, which occurred in February 2023. An abstract was submitted to the 2023 Military Health System Research Symposium, “Sustained Dynamic Compression Device Provides Continuous Compression in the Setting of Bone Resorption Following Arthrodesis in an Ovine Model.” The abstract was accepted for a poster presentation, which occurred in August 2023.

6.2 Website(s) or other Internet site(s)
Nothing to Report

6.3 Technologies or techniques
From this research, a new animal model of arthrodesis has been developed, specifically calcaneal-tarsal-metatarsal fusion in an ovine model. A device is placed antegrade through the calcaneus into the metatarsal, then fixated in both the metatarsal and the calcaneus with transverse screws. The surgical technique itself follows that used clinically in humans for hindfoot and midfoot fusion. The technique has been successfully adapted to an ovine model, which allows for further biomechanical and bone biology research to be conducted. Research involving this technique and animal model will be shared at future Orthopaedic Research Society meetings and Military Health System Research Symposiums.

6.4 Inventions, patent applications, and/or licenses
Nothing to Report

6.5 Other Products
Medical Device:
The outerbodies of the dynamic prototype device went through multiple design iterations in Year 1. Ultimately, a design with a tapered threaded end for bone fixation that matched closely to the size of the proximal intramedullary canal of the 4th metatarsal was chosen as the final design. The other end of the device utilizes a transverse screw like other intramedullary devices. Overall lengths were chosen to range from 110 mm to 140 mm to span the length of the lateral column using a posterior surgical approach. Future project activities include regulatory submission to the FDA so that the prototype device can be used clinically, especially in at-risk patients, especially the Veteran population, who are not being adequately treated using existing static internal fixation technology. Project results to date show that the prototype device will be substantially equivalent to competitor devices already cleared by the US FDA.

7. Participants & Other Collaborating Organizations
7.1 Individuals on Project

Name:	David Safranski
Project Role:	PI
Research Identifier:	0000-0001-5722-5831
Nearest Person Month:	2

Contribution to Project:	Dr. Safranski has managed overall project, device design, protocol development, quality monitor of testing, data management, and management of subawardee.
Funding Support:	N/A

Name:	Ken Dupont
Project Role:	Senior Personnel
Research Identifier:	
Nearest Person Month:	1
Contribution to Project:	Dr. Dupont has worked on the quality management system documentation, review of animal studies, and report preparation.
Funding Support:	N/A

Name:	Claudia Vitale
Project Role:	Co-operative student/Intern
Research Identifier:	
Nearest Person Month:	1
Contribution to Project:	Ms. Vitale has worked on protocol development and biomechanical testing of devices, and data processing.
Funding Support:	N/A

Name:	Jack Griffis
Project Role:	Senior Personnel
Research Identifier:	
Nearest Person Month:	1
Contribution to Project:	Mr. Griffis has worked on regulatory and quality management system documentation and reports.
Funding Support:	N/A

7.2 Active Support of PI and Key Personnel
Nothing to Report.

7.3 Subawardee Organization
The Presurgical Research Laboratory and the Orthopaedic Bioengineering Research Laboratory at Colorado State University are serving as the subawardee for this research grant, where they will perform the *in vivo* animal model and subsequent analysis.
Organization: Colorado State University
Location: Fort Collins, Colorado
Contribution: Research facilities and research collaboration as a subawardee to perform the animal model.

8. Special Reporting Requirements

Nothing to Report

9. Appendices

9.1 List of Abbreviations and Acronyms

ACURO – Animal Care and Use Review Office

ASTM – American Society for Testing and Materials

BV – Bone Volume

CAD – Computer Aided Drafting/Design

CSU – Colorado State University

CT – Computed Tomography

FDA – (United States) Food and Drug Administration

HA – hydroxyapatite

IACUC – Institutional Animal Care and Use Committee

ICD-10-PCS – International Classification of Diseases, 10th Edition, Procedure Codes

IRB – Institute Review Board

kGy - kilogray

MDBV – Mean Density of the Bone Volume

m – meter

MHSRS - Military Health System Research Symposium

micro-CT or µCT - Micro-computed Tomography

mm - millimeter

MTS – Materials Test Systems

N - Newton

NiTi – Nickel Titanium (alloy)

PCF – Pounds per Cubic Foot (density)

SAL – Sterility Assurance Level